INVESTIGATING THE APPLICABILITY OF THE COMPENSATORY RESERVE INDEX FOR FORECASTING INTRACRANIAL PRESSURE EVENTS

By

BIANCA PINEDA

A thesis submitted to the

Graduate School – New Brunswick

Rutgers, The State University of New Jersey

In partial fulfillment of the requirements

For the degree of

Master of Science

Graduate Program in Biomedical Engineering

Written under the direction of

WILLIAM CRAELIUS

And approved by

_____

_____

_____

_____

New Brunswick, New Jersey

[October 2015]

ABSTRACT OF THE THESIS

Investigating the Applicability of the Compensatory Reserve Index for Forecasting Intracranial Pressure Events

by BIANCA PINEDA

Thesis Director:

William Craelius

There are about 1.7 million cases of traumatic brain injury in the U.S. annually. After injury, the body's compensatory mechanisms cause fluid to accumulate in the cranium. This gives rise to elevated intracranial pressure (ICP) which then causes ischemia. To compensate for this, vessels dilate causing more fluid to build and the cycle to repeat. If left unchecked, this cycle compromises cerebral autoregulation such that the body cannot maintain stable ICP in response to changes in volume. This leads to intracranial hypertension and secondary injuries such as hemorrhaging, etc. In order to prevent secondary injury, the standard of care for patients with moderate to severe head injuries is to monitor their ICP in surgical intensive care units. However, treatments are only implemented after ICP has reached a critical value and noticeable damage has occurred. The goal of this project is to develop a method to forecast the occurrence of these critical events in ICP so that treatments can be applied preemptively.

Working towards this goal, a numerical descriptor of cerebral autoregulation called the compensatory reserve index (RAP) was analyzed for its potential ability to forecast rises in ICP. Retrospective data was analyzed from two patients with TBI who were monitored for 38 and 340 hours, respectively. Hours were separated into either 'stable' or 'unstable' periods of ICP according to established rules and RAP calculated for each hour. Results showed that, 1) the cumulative distribution of RAP calculated in 'stable' ICP periods differs significantly from that in 'unstable' periods ($p < 0.001$), 2) in several instances of ICP elevation, RAP exceeded the set threshold in both patients with latency values normally between 1-3 minutes. Thus, the results support the hypothesis that RAP is significantly associated with hemodynamic instability and its potential as a predictor of the same.

Acknowledgements

I would like to acknowledge and thank the following people who have made the completion of this thesis possible:

Dr. William Craelius, mentor, for all his guidance, support, and encouragement during both my undergraduate and graduate studies.

Maria Qadri, graduate student, for always having time for questions and advice despite being busy

Colin Kosinski, graduate student, for the helpful insights, questions, and comic relief

Dr. Nam Kim, post-doctoral fellow, for helping me get started on the project and being willing to answer all of my questions

Dr. Shabbar Danish, for cooperating with our lab and allowing us to collect and analyze patient data from Robert Wood Johnson University Hospital

Drs. Ilker Hacihaliloglu, Hilton Kaplan, and John Khan, members of my thesis committee, for all the helpful feedback towards my thesis.

The *New Jersey Commission on Brain Injury Research*, for their generous support and funding for this project

My *family and friends*, for their love and support

Table of Contents

Abstract ii

Acknowledgements iv

Table of Contents v

List of Tables vii

List of Illustrations vii

Abbreviations xi

Introduction 1

I. Population 1
II. Current Problems, Challenges, and Needs 2

Literature Review 4

I. Monro-Kellie Doctrine and Pathophysiology 4
II. Cerebrovascular Autoregulation 5
III. Cerebral AR Models 6
IV. The Compensatory Reserve Index (RAP) 7

Hypothesis 10

Methods 11

I. Gathering Data 12
II. Data Validation 13
III. Data Pre-processing 14

Table of Contents cont'd

IV. RAP Calculation 16
V. Distribution Analysis 17
VI. Comparison and CRPs: ICP vs. RAP, AMP vs. mICP 18

Results and Discussion 19

I. Comparison of Simulated vs. Real ICP Data 19
II. Comparison of Stable vs. Unstable Distributions 21
III. Latency Between RAP Increase and ICP events 22
IV. ICP vs. RAP 23
i. Simulated ICP Data 24
ii. Hours 22-24 : ICP vs. RAP in TBI Patient 1 24
iii. Subsequent Hours 25-27 : ICP vs. RAP in same TBI Patient 1 26
iv. Hours 62-63 : ICP vs. RAP in TBI Patient 2 27
v. Hours 127-129 : ICP vs. RAP in TBI Patient 2 29
V. Mean vs. Amplitude of ICP 31

Future Work 34

Conclusions 35

Appendices 36

I. Appendix A 36
II. Appendix B 37
III. Appendix C 38
IV. Appendix D 39
V. Appendix E 40

References 41

Acknowledgement of Previous Publications 45

List of Tables

Table 1: Summary / description of each stage of the intracranial PV curve 9

List of Illustrations

Figure 1: Cascade of events within the skull after primary insult. High / dangerous levels of ICP defined as > 20 mmHg 2

Figure 2: Stepwise Approach to the Management of ICP / Cerebral Perfusion Pressure (CPP)-Guided Therapy: treatment initiated to maintain ICP > 20 mmHg and CPP > 60 mmHg. Adapted from [7] 3

Figure 3: After TBI, this cycle amplifies ICP and volume until cerebral AR is compromised – thereby causing secondary injury 4

Figure 4: Intracranial PV curve with stages described in Table 1. RAP reflects the relationship between the volume of intracranial space and ICP. Typically RAP is high in magnitude and positive following head injury. Adapted from [34, 52].....9

Figure 5: Data collected via analog outputs from the back of a TRAM housing unit: GE Tram-rac 4A; analog outputs were collected using NI-USB 6210 DAQ; signal was sampled at 50 Hz, with a resolution (absolute accuracy) of 1.41 mV at ±5 V analog input range, which is equivalent to the pressure resolution of 0.141 mmHg, and capable of detecting ±500 mmHg range.....12

Figure 6: Data being collected by CHARM was correlated with the signals obtained from hospital monitors and showed a cross correlation of 1.00 13

Figure 7: Example of raw vs. processed ICP data prior to RAP calculation. Non-relevant data were filtered out by applying a moving window that removed segments that exceeded a set threshold of ICP and dICP (slope) 14

Figure 8: ICP signal before and after application of Butterworth low-pass filter 15

Figure 9: FFT of ICP. The y value of the highest peak within the frequencies of 1-4 Hz was used as the pulse amplitude (AMP) value for every 300 pt. (6 sec.) window 16

Figure 10: a,c) segments of filtered ICP signal (a: 6 sec; b: 5 min); b,d) segments of simulated ICP signal generated (c: 3 sec; d: 5 min). Note: difference in rates (a,b) 19

Figure 11: Calculated RAP (4 hrs) for simulated ICP signal ($\sigma^2 = 0.0234$). Note: variance is occurring at a higher frequency compared to real ICP data due to noise. Constantly low RAP values (near 0) at low ICP mean that this signal would theoretically be stable 20

Figure 12: Calculated RAP (1 hr) for measured ICP signal from TBI patient ($\sigma^2 = 0.0675$). Higher variance observed due to unstable ICP 20

Figure 13: a) Probability distribution of unstable (red) vs. stable (blue) ICP data. b) Probability distribution of unstable (red) vs. stable (blue) RAP data (Patient 1). The black reference line at 0.5 marks the threshold chosen for categorizing events as unstable. 21

Figure 14: Patient 2, Hr 7 – RAP crosses the threshold and stays positive approx. 3 minutes before an event occurs in ICP. 22

Figure 15: Patient 1, Hr 25 – RAP crosses the threshold approx. 30 seconds prior to the event 23

Figure 16: The CRP has been separated into regions based on thresholds demarcated by the red lines. Any values in the red regions mean that the patient is very unstable (due to high values of ICP coupled with a high RAP magnitude). Values in the blue region mean that the patient is most likely stable (due to low ICP coupled with low amplitude values) [32, 34]. Values in any other areas are indeterminate.....23

Figure 17: a) 1 hour of simulated ICP and calculated RAP values, b) scatter plot of ICP vs. RAP values for simulated ICP in (a).....24

Figure 18: Patient 1; 3 – 1 hour consecutive segments from 22nd -24th hours shows the distribution ICP and RAP before (a-b), during (c-d), and after (e-f) an unstable period. (a,c,e) 0.5 RAP threshold shown as dotted line with unstable RAP in red. Note: ICP data down-sampled to size of RAP for scatter plots.....25

Figure 19: Patient 1; Subsequent 3 hour timespan (25th -27th) shows stabilization 2 hours after an event (a-b). (c-d) illustrate that despite the appearance of low stable ICP, RAP values may stay high for a prolonged period before stable RAP values are reached (e-f) 26-7

Figure 20: Patient 2; 3 hour timespan (61st -63rd) shows ICP and RAP before (a-b), during and after an event (a-b). Increased ICP is observed with low RAP, but ICP decreases after the event (c-d) and RAP maintains mostly positive values for subsequent hours (c-f)..... 28-9

Figure 21: Patient 2; 3 hour timespan (127th -129th) shows increase in RAP despite low ICP prior to event (a-b) consistently high RAP during the event (c-d) and delayed RAP stabilization as ICP decreases below threshold after the event (e-f) 30

Figure 22: Patient 1; 2 consecutive hours (14^{th} -15^{th}) where a breakpoint or change from positive (a-b) to negative (c-d) slope, was found in plotted amplitude vs. mean ICP data. (a) 14^{th} hour ICP and RAP data (b) amplitude and mean ICP data from that hour plotted against each other with a linear fit; slope = 0.10081 (c) 15^{th} hour ICP and RAP data (d) amplitude and mean ICP data from that hour plotted against each other with a linear fit; slope = -0.05813 32

Figure 23: Patient 2; 2 consecutive hours where a breakpoint or change from positive (a-b) to negative (c-d) slope, was found in plotted amplitude vs. mean ICP data. (a) 62nd hour ICP and RAP data (b) amplitude and mean ICP data from that hour plotted against each other with a linear fit; slope = 0.18374 (c) 63rd hour ICP and RAP data (d) amplitude and mean ICP data from that hour plotted against each other with a linear fit; slope = -0.041393 33

Abbreviations

TBI – Traumatic Brain Injury

ICP – Intracranial Pressure

ICU / SICU – (Surgical) Intensive Care Unit

GCS – Glasgow Coma Score

CT – Computed Tomography

HOB – Head of Bed

CPP – Cerebral Perfusion Pressure [CPP = MAP - ICP]

CSF – Cerebrospinal Fluid

IH – Intracranial Hypertension

AR – Autoregulation

CBF – Cerebral Blood Flow

ABP – Arterial Blood Pressure

MAP – Mean Arterial Pressure

PRx – Pressure Reactivity Index

PAx – Pressure Amplitude Index

FFT – Fast Fourier Transform

MOICAIP – Morphological Clustering and Analysis of ICP Pulse

RAP – Index of Compensatory Reserve

AMP – Pulse Amplitude of ICP

mICP – Mean of ICP

CHARM – Continuous Hemodynamic Autoregulation Monitor

ECG – Electrocardiogram

PAR – Phase Area Ratio

RWJUH – Robert Wood Johnson University Hospital

HIPAA – Health Insurance Portability and Accountability Act

FIFO – First In, First Out

CRP – Compensatory Reserve Plot

Introduction

Traumatic brain injury (TBI) occurs when a mechanical impact or trauma to the head causes a closed or penetrating injury which results in the deformation of brain tissue. Depending on the nature, speed, and location of the impact—the injury can range anywhere from a mild concussion to an extended loss of consciousness [1].

I. Population

TBI is the leading cause of death and disability worldwide [2]. The risk of TBI is especially high among adolescents, young adults, and people older than 75 years [3]. However, in reality TBI can happen to anyone, anywhere, anytime. The top causes of TBI include accidents, falls, and sports injuries with falls being the leading cause of traumatic brain injury for all ages [4]. At least 5.3 million Americans are currently living with disabilities resulting from TBI. Most of whom have a 2.3-4.5 times increased risk of Alzheimer's disease. In addition, Veterans' advocates believe that between 10 and 20% of Iraq veterans (150,000 and 300,000 service members) have some level of TBI due to exposure to blasts in war zones [5, 6].

II. Current Problems, Challenges, and Needs

The problem with TBI is that there is a likelihood of secondary injury which can manifest in the hours, days, and weeks following the initial trauma [7]. Often, secondary injuries to the brain can be more dangerous than primary injuries because they linger and progressively get worse without treatment. Several factors contribute to the formation of secondary injuries post-TBI such as hypoxemia, hypotension, intracranial hemorrhage, and especially increased intracranial pressure (ICP) [1]. ICP is the primary predictor of outcome following TBI and is closely monitored in patients (Fig. 1). Outcomes directly relate to the control of intracranial pressure (ICP) [8-10]. This is because the increased fluid pressure (due to cerebrospinal fluid influx) leads to swelling, which impairs cerebral blood flow and causes further ischemic tissue damage [7].

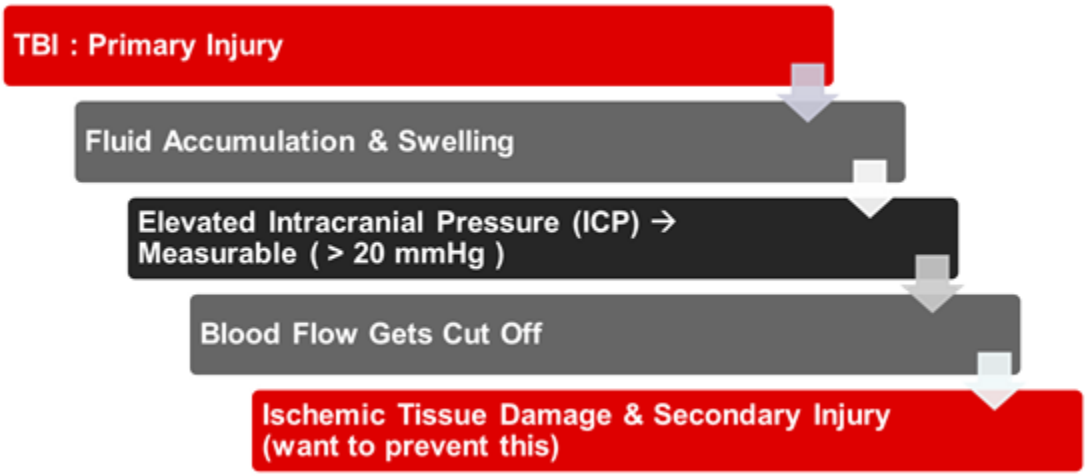

Figure 1: Cascade of events within the skull after primary insult. High / dangerous levels of ICP defined as > 20 mmHg

In order to prevent secondary insults, patients are often transferred to an intensive care unit (ICU) for neurocritical care management. ICP monitoring is indicated for patients with moderate to severe traumatic brain injury and a Glasgow Coma Scale (GCS) score of less than or equal to 8 with an abnormal computed tomography (CT) scan. Current treatment measures for elevated ICP include: patient positioning—where elevation of the head of the bed (HOB) from 0 to 30° significantly decreases ICP, hyperosmolar therapy—where drugs such as Mannitol are delivered, and cerebrospinal fluid drainage (Fig. 2). Regardless, admission to an ICU does not eliminate the occurrence of secondary insults [7].

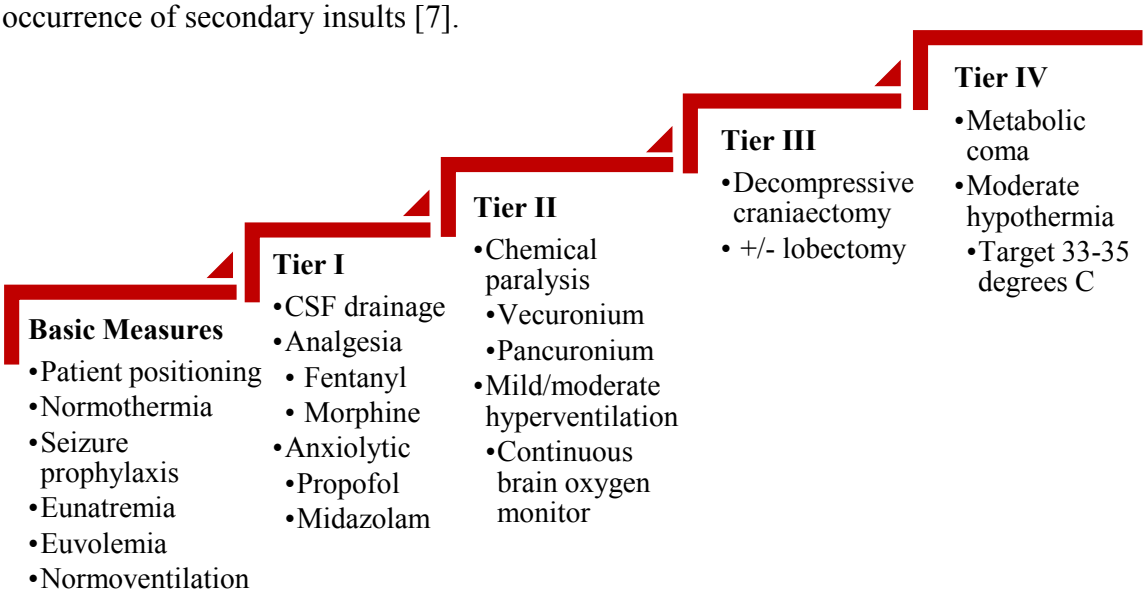

Figure 2: Stepwise Approach to the Management of ICP / Cerebral Perfusion Pressure (CPP)-Guided Therapy: treatment initiated to maintain ICP > 20 mmHg and CPP > 60 mmHg. Adapted from [7]

The problem with the outlined approach is that therapeutic decisions are made after ICP elevation and subsequent damage has already occurred. Thus, the overall goal of this project is to engineer a device / develop metrics that can provide continuous and accurate predictive information in order to improve therapeutic outcomes for TBI. This will enable treatments to be preventive rather than corrective.

Literature Review

I. Monro-Kellie Doctrine and Pathophysiology

The Monro-Kellie doctrine states that the cranium (and spinal canal) can be thought of as a closed, rigid container with a constant volume. Therefore, the sum of the volumes of the brain, intracranial blood, and cerebrospinal fluid is constant. Furthermore, assuming that the contents are incompressible, this implies that changes in volume in one component will cause a reciprocal change in volume in the other components [11].

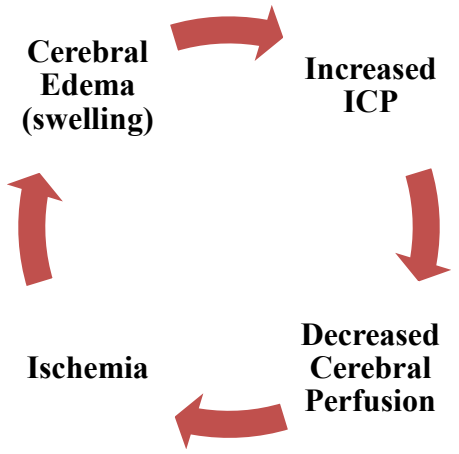

Figure 3: After TBI, this cycle amplifies ICP and volume until cerebral AR is compromised – thereby causing secondary injury.

After a patient is subjected to TBI, the body's normal healing response will cause fluid (CSF) to accumulate in the intracranial space – thereby elevating the ICP. Since total volume is constant, this increase in CSF causes a decrease in venous/arterial blood volume [12]. As a consequence there is decreased cerebral perfusion and ischemia. Due to the lack of blood flow, the body compensates by increasing vessel compliance (vasodilation). Unfortunately, this compensatory mechanism causes pressure (ICP) to increase further.

This compensatory cycle (Fig. 3) can cause intracranial hypertension (IH) and secondary injuries such as ischemic tissue damage and brain stem herniation if left unchecked. Due to this pressure-volume relationship, CSF drainage is often used to decrease ICP. In fact, draining as much as 3 ml of fluid was found to decrease ICP by 10.1% (relative to the baseline value) for 10 min [13].

II. Cerebrovascular Autoregulation

Cerebrovascular autoregulation (AR) is the underlying mechanism responsible for managing cerebral perfusion and ICP. This is done by varying the resistance of blood vessels (through either vasodilation or vasoconstriction) in response to changes in blood pressure and by maintaining constant cerebral blood flow (CBF) rate in order to keep tissues constantly oxygenated. Impairment of cerebrovascular AR increases the risk for secondary brain damage [14]. Thus, predicting the behavior of this complex physiological control system is essential to rational treatment of its breakdown following TBI.

Considering its importance, many laboratories are searching for accurate predictors for AR [15-23]. The most common approaches can be divided into two categories: (1) models, which combine several parameters into a single index/prediction, and (2) waveform analysis, which uses evolving ICP pulse waveform features as predictors of future values. This paper will focus primarily on the compensatory reserve index – which falls into the first category of cerebral AR models.

III. Cerebral AR Models

Models derive indices of the internal state of the AR system from physiological parameters that are measured in TBI patients such as ICP and arterial blood pressure (ABP). For example, CPP measures the net pressure gradient causing cerebral blood flow to the brain and is the simplest / most clinically used index. CPP is defined as CPP = MAP – ICP (expressed in mmHg) where MAP is the mean arterial pressure (typically averaged over 5 minutes). The problem with CPP is that there is no established optimal CPP following TBI due to limited Class 1 study data indicating an optimal CPP threshold for TBI. However, data from a few studies do indicate that cerebral blood flow declines to ischemic range when CPP varies between 50-60 mmHg [24]. Other commonly used models include: the pressure reactivity index (PRx) which is defined as the least square regression slope of ICP and MAP (over 20 minute periods), the Mx index which is based on CBF from transcranial Doppler signal, cerebral blood oxygenation using near infrared spectroscopy, and arterial CO_2 [15, 19-21, 25]. However, since one metric may not apply to all cases, dynamic, multicomponent models have been used to assess AR both retrospectively and prospectively. These models have accurately predicted (retroactively) AR responses to manipulations such as HOB, using recorded data from TBI patients [23, 26].

IV. The Compensatory Reserve Index (RAP)

As previously discussed, there is a relationship between ICP and intracranial volume. However, due to the cyclic compensatory mechanisms at play, it is difficult to tell how far along a patient is before complete loss of cerebral AR and damage occurs. The index of compensatory reserve is a cerebral AR model that characterizes the pressure-volume relationship. It is otherwise known as RAP because it is the correlation (R) between the pulse amplitude of the ICP (A) and the mean of the ICP (P) –where the pulse amplitude (AMP) is the slope of the intracranial pressure-volume (PV) curve (Fig. 4) [34-5]. In order to understand RAP and how it can be used, it is essential to understand the associated pressure-volume curve and its physiological translation.

The pressure-volume curve can be divided into three stages. In the first stage, RAP ~ 0 which means that the pulse amplitude is not correlated with mean ICP (mICP). At this stage cerebral AR is still intact because changes in intracranial blood volume do not cause rapid changes or large fluctuations in ICP. As volume and pressure increase (typical in a brain injury and IH), the curve approaches stage 2. At this stage, RAP is high and positive (~ 1) which means that pulse amplitude varies along with mICP. As illustrated (Fig. 4), when RAP is positive and ICP is high, small changes in volume can cause large fluctuations in ICP. Physiologically, this indicates poor compensatory reserve / AR as well as decreasing compliance as vessels dilate in response to increasing pressure and volume. As ICP values reach a critical threshold (~ 50-80 mmHg), RAP starts to become negative as the curve proceeds to stage 3 [31]. Here, the pulse amplitude decreases as ICP increases.

This occurs because the vessels lose the capacity to dilate any further and instead collapse under high pressure. At this stage, there is complete loss of AR and compensatory reserve.

As demonstrated, the pressure volume curve is such that low pulse amplitude is observed both in stages 1 and 3. Thus, by correlating the pulse amplitude to mICP (i.e. RAP), it is easier to tell how the two are interacting and where on the curve one is at. Numerous studies have shown that RAP is indicative of patient outcome. For example, at high ICP values, a sign change in RAP from positive to negative (breakpoint) was observed in patients with a fatal outcome [32, 34-5]. Studies have also shown that RAP changes in response to decompressive craniectomy, hyperventilation, body position, shunting, infusion studies, and even during sleep [33, 36-7].

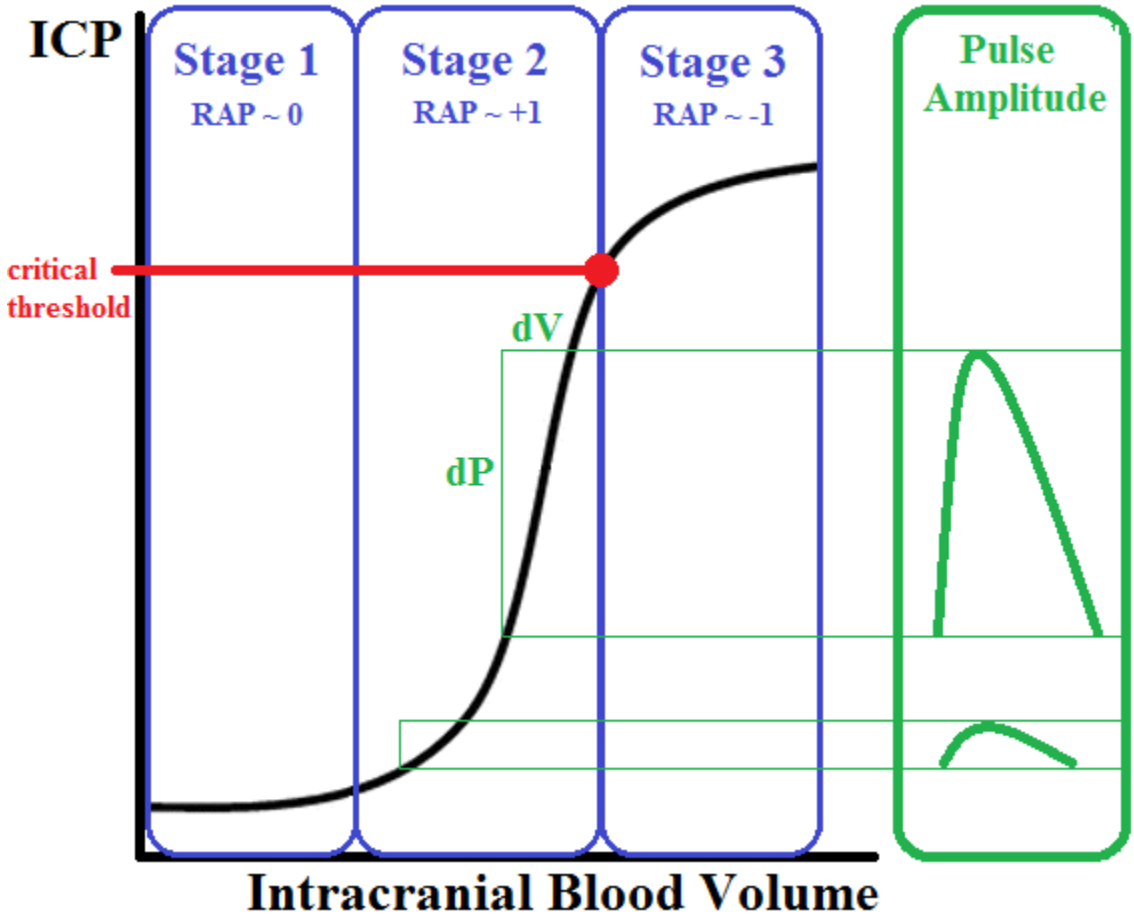

Figure 4: Intracranial PV curve with stages described in Table 1. RAP reflects the relationship between the volume of intracranial space and ICP. Pulse amplitude (AMP) represents the slope of the PV curve. Typically RAP is high in magnitude and positive following head injury. Adapted from [34, 52]

Table 1: Summary / description of each stage of the intracranial PV curve

Stage 1	RAP ~ 0 • AMP and mICP not synchronized	ΔV → small ΔICP (low pulse amplitude) • Good compensatory reserve • AR intact, stable
Stage 2	RAP ~ +1 • AMP varies with mICP	ΔV → rapid ΔICP (high pulse amplitude) • Poor AR / compensatory reserve
Stage 3	RAP ~ -1 • AMP decreases as mICP increases	• Low pulse amplitude • Maximally dilated vessels → collapse from high pressure • No cerebral AR / compensatory reserve

Hypothesis

RAP has been used in other studies to assess cerebrospinal fluid dynamics in hydrocephalus/head injury, determine the value of overnight monitoring of ICP, and observe the effect of craniectomy on ICP [36, 42-44]. However, there is still currently no consensus in literature on the forecasting reliability of the RAP index. In addition, literature reveals no direct comparisons of the relationship of ICP vs. RAP on the same graph. Rather, RAP has mostly been studied in relation to outcome [34-37, 40-50]. Thus, keeping the PV curve in mind, it is hypothesized that a graphical comparison of the calculated RAP with monitored ICP values will help simplify and map out how unstable a patient is and how close they are to complete loss of cerebral AR. It is further hypothesized that investigating elevated 'events' in ICP can provide evidence that the RAP index is associated with hemodynamic instability. This can help determine the potential of RAP for forecasting.

Methods

A module was developed in order to siphon, compress, and store signals from existing monitors in the surgical intensive care unit (SICU). This module, called the continuous hemodynamic autoregulation monitor (CHARM), can also be programmed to search for statistical relationships between any proposed index and adverse events. Over an 18 month period, CHARM has collected continuous records of ABP, ICP, electrocardiogram (ECG), blood oxygen level and respiration from 29 patients with TBI. Overall, the goal is to examine possible relationships among the various AR indices. Thus far, three different indices have been investigated: the PRx which is a commonly used AR index, the phase-area ratio (PAR) score (newly developed), and RAP which is the focus of this study. Once an optimized set of indices/algorithms have been developed – they will be weighted, consolidated into one index, programmed into CHARM, and tested with real-time patient data.

I. Gathering Data

ICP signals were collected from patients with TBI who are being monitored in the SICU of Robert Wood Johnson University Hospital (RWJUH). Data were gathered from standard clinical monitors routinely used in the SICU (Fig. 5) without interfering in patient monitoring. In addition, the study was approved by the Rutgers IRB and all data were de-identified to eliminate risks of unauthorized disclosure of personal identifiers (in accordance with HIPAA).

Figure 5: Data collected via analog outputs from the back of a TRAM housing unit: GE Tram-rac 4A; analog outputs were collected using NI-USB 6210 DAQ; signal was sampled at 50 Hz, with a resolution (absolute accuracy) of 1.41 mV at ±5 V analog input range, which is equivalent to the pressure resolution of 0.141 mmHg, and capable of detecting ±500 mmHg range

ICP was continuously monitored with intraparenchymal microtransducers (Camino Direct Pressure Monitor). In some patients, ICP data were intermittently available from ventriculostomy procedures.

II. Data Validation

Data validation was completed by cross-correlating the CHARM data acquisition unit data stream with that from the hospital SICU monitor. The result was adequate cross correlation between the two signals (Fig. 6). Therefore, it was concluded that the data obtained from the CHARM units were valid. Modules for identifying channels, artifact rejection, and peak detection have also been programmed and tested [38]

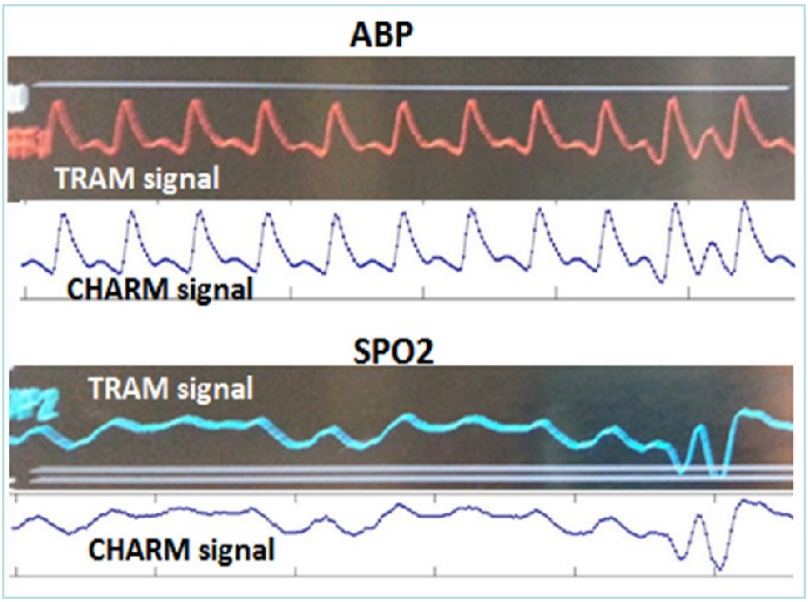

Figure 6: Data being collected by CHARM were correlated with the signals obtained from hospital monitors and showed a cross correlation of 1.00

III. Data Pre-processing

One of the initial challenges encountered was differentiating between usable patient ICP data and abnormal data due to sensor dislodgement/disconnection, etc. One measure that was taken to help remedy the problem was setting thresholds on the data—where any segments (length = 3 s) with ICP values that were negative or greater than 80 mmHg were determined to be non-relevant physiological signals and removed. These thresholds were set based on feedback from Dr. Danish and normal physiological ICP values [39]. Additional feedback also revealed that changes in ICP that are not sustained are usually ignored by nurses due to the fact that they could be caused by events such as a patient coughing, etc. Thus, instantaneous changes in ICP were also filtered out by removing segments (of length = 3 sec) where the derivative of ICP (dICP) is less than -1 or greater than 2 (Fig. 7). These values were determined by comparing the distribution of valid vs. invalid ICP data (Appendix A).

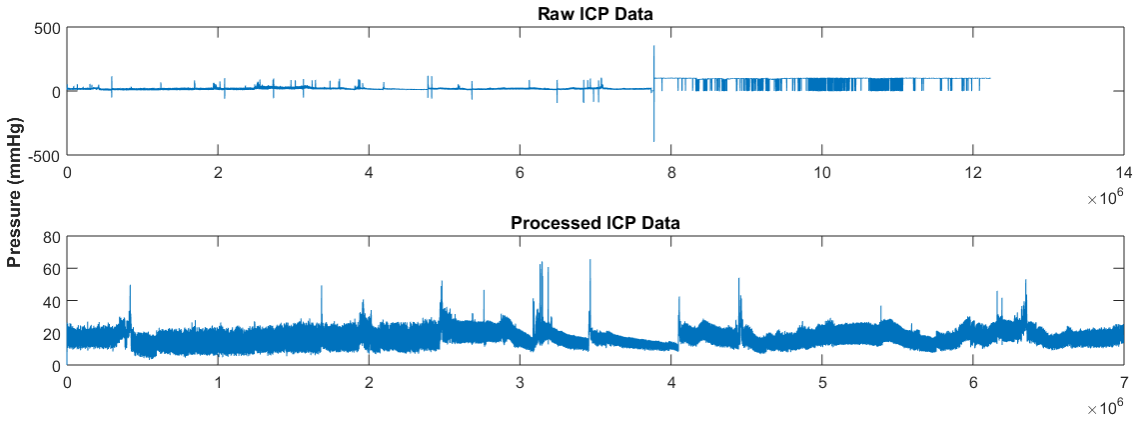

Figure 7: Example of raw vs. processed ICP data prior to RAP calculation. Non-relevant data were filtered out by applying a moving window that removed segments that exceeded a set threshold of ICP and dICP (slope)

After invalid segments were removed, a Butterworth low-pass filter was used to smooth the data and remove noise from non-relevant frequencies (Fig. 8). The filter parameters were determined from frequency values found experimentally and in literature [39]. The parameters used were as follows: 4 Hz passband frequency, 5 Hz stopband frequency, 1 dB passband ripple, 5 dB stopband attenuation (for data sampled at 50 Hz).

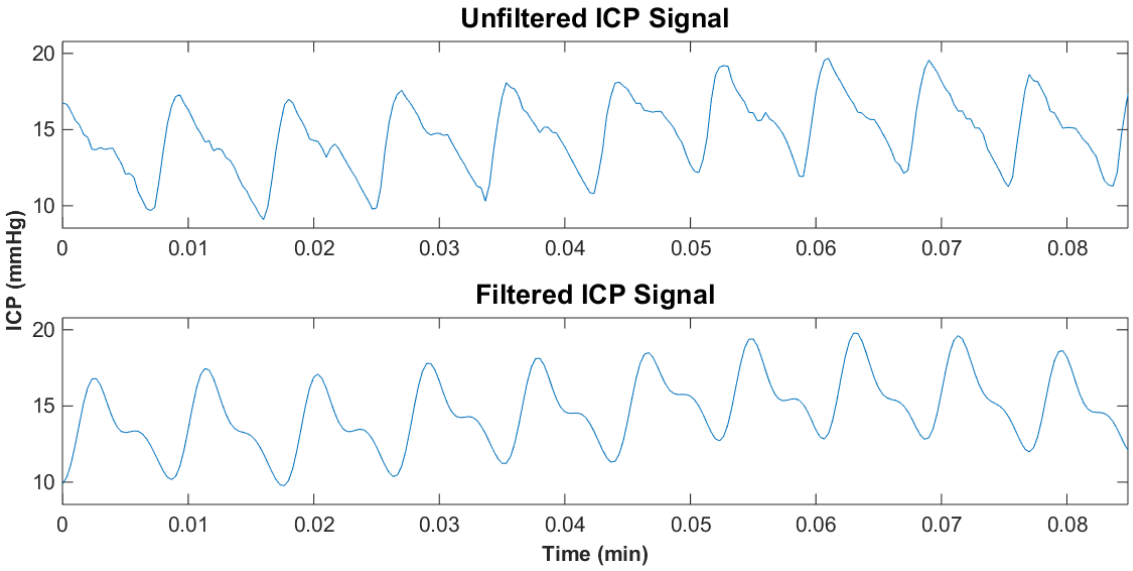

Figure 8: ICP signal before and after application of Butterworth low-pass filter

IV. RAP Calculation

Calculation of the RAP index was adapted from previous methods [34-7, 39-40]. In order to calculate mICP and AMP, a 300 pt. moving window (rectangular, no overlap) was applied to the filtered ICP data. mICP was obtained by using the mean ICP value of every window. In order to calculate AMP, an FFT was obtained for every 300 pt. window. The amplitude of the first fundamental harmonic component (AMP) was then isolated by extracting the maximum value between 1 and 4 Hz (Fig. 9). Although, this method consistently yields values lower than the peak to peak amplitude, it is equivalent to time domain analysis, better correlates with mean ICP, and minimizes the influence of noise and measurement errors [32, 41].

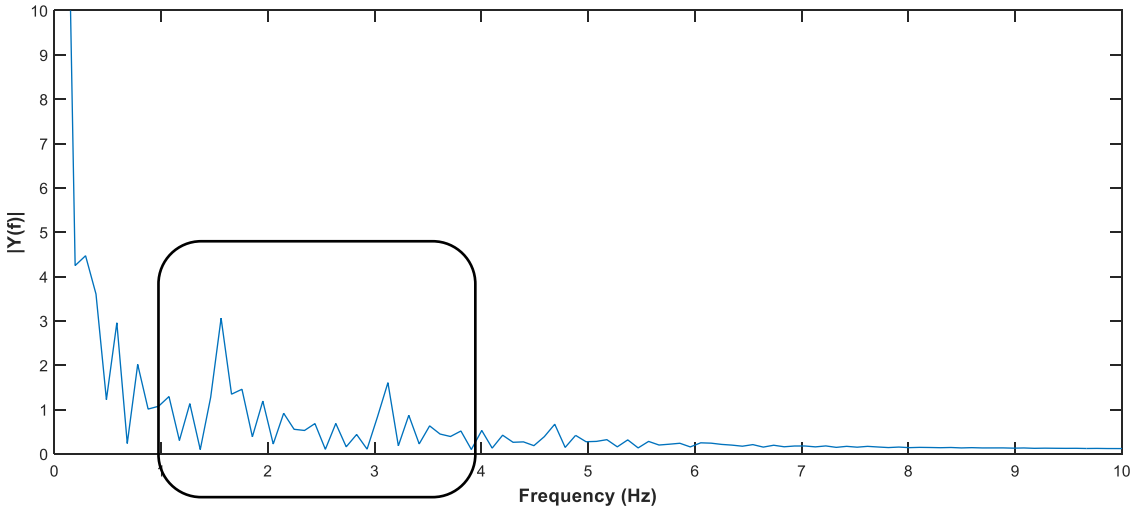

Figure 9: FFT of ICP. The y value of the highest peak within the frequencies of 1-4 Hz was used as the pulse amplitude (AMP) value for every 300 pt. (6 sec.) window.

The RAP index was obtained by computing the linear correlation between the amplitude and mean of the ICP data. A RAP value was calculated for every 40 subsequent values of mean AMP and mICP using a first in, first out (FIFO) method. RAP values were then calculated for simulated and real ICP data for comparison (Fig. 10-12, Appendix B).

V. Distribution Analysis

When it comes to ICP, there is no absolute agreement on the threshold level at which treatment should be administered. In reality, it varies depending on age and disease type. For example, in hydrocephalus, values > 15 mmHg are regarded as elevated. On the other hand, for head injured adults, the threshold is between 20-25 mmHg [50]. Similarly, there is no universally accepted threshold for RAP values. In order to determine appropriate thresholds for stable vs. unstable ICP/RAP values, an event finder was used to demarcate unstable segments in ICP. The event finder works by obtaining the ICP trend through the application of a low-pass filter (1-2 Hz) followed by a least squares polynomial fit (1^{st} order). When the slope of the trend exceeds a value of 0.15 (values range from 0.1 to 0.2), the associated ICP segments were marked out and plotted. This allows for a visual indicator of unstable ICP events (Fig. 15-7).

The event finder was applied to 38 hours of ICP data recorded from a patient that was admitted with TBI (GCS = 4) and eventually discharged for rehabilitation (GCS = 14 at discharge). First, the data were separated into 1 hour segments. Then RAP was calculated for each hour. Finally, ICP and their associated RAP segments were categorized as stable if they contained no events and unstable if they contained events. The distribution of stable vs. unstable ICP and RAP were then plotted and the nearest probability distribution fit applied (Fig. 13, Appendix C).

VI. Comparison and CRPs: ICP vs. RAP, AMP vs. mICP

First, ICP vs. RAP was plotted for simulated data (Fig. 17). Then, data from 2 patients was used to investigate the relationships between RAP and ICP. Patient 1 was as previously described in section (V) of methods. Patient 2 was also admitted with TBI and later discharged for rehabilitation, but was monitored for a longer amount of time (340 hrs). First, ICP and RAP were plotted separately to investigate the latency between RAP and ICP events (Fig. 14-5). Then, using the experimentally determined thresholds for ICP and RAP (Fig. 16), mean ICP and RAP data were plotted against each other (via scatter plot) for every hour of data to investigate possible relationships (Fig. 18-21). The resulting scatter plots will be referred to as compensatory reserve plots (CRP). Note that ICP data were down-sampled to the size of the RAP segment for each hour. Thus, the density of ICP points is equivalent to that of the RAP. In addition to the aforementioned, the amplitude vs. mean ICP were also plotted for every hour and fitted with a linear trend line (Fig. 22-3) to investigate any possible breakpoints (changes from positive to negative RAP).

Results and Discussion

I. Comparison of Simulated vs. Real ICP Data

In order to determine whether the RAP calculation was running properly, it was used on both simulated and real ICP data (Fig. 10) where the simulated data was programmed to have constant amplitude and mean (Fig. 11). Note that the simulated AMP and mICP appear relatively smooth, but both contain 40 dB magnitude white noise (Appendix B).

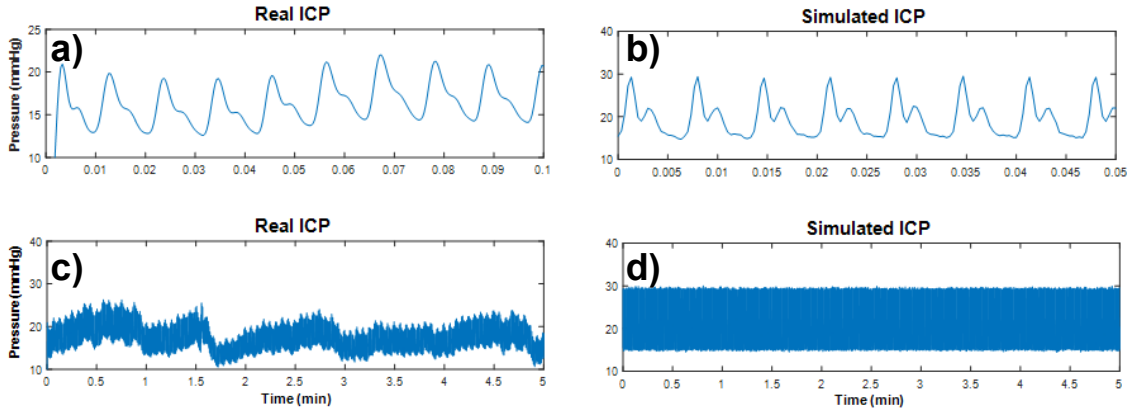

Figure 10: a,c) segments of filtered ICP signal (a: 6 sec; b: 5 min); b,d) segments of simulated ICP signal generated (c: 3 sec; d: 5 min). Note: difference in rates (a,b)

Figure 11 shows that the RAP calculation correctly estimates both the amplitude and mean of the simulated signal. As expected, using the FFT method means that the amplitude estimation is always consistently lower than the peak to peak amplitude (previously discussed). In addition, it can be observed that the calculated RAP for the simulated signal yields consistently low values for a low mean ICP of approximately 20 mmHg which is what would be expected for a constant, stable signal. The calculated variance was 0.0234. Small fluctuations may be due to the noise added to the signal.

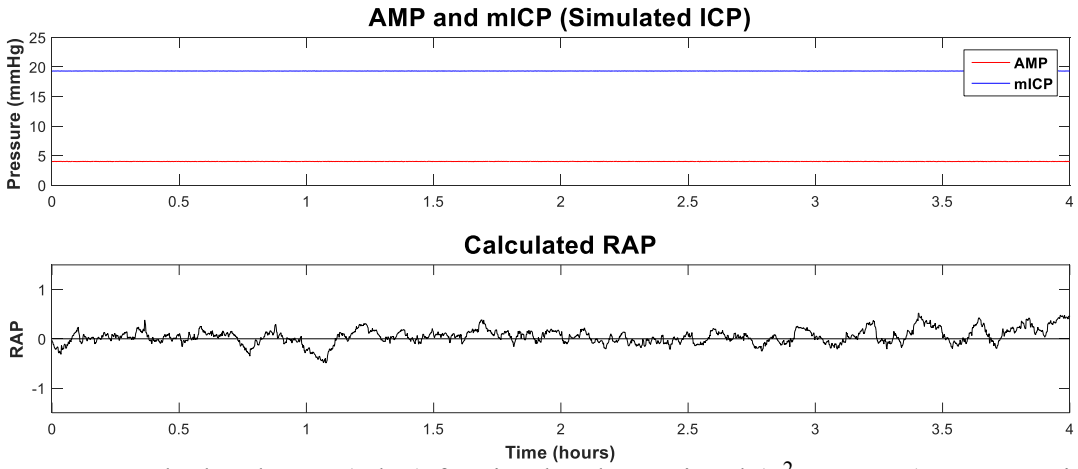

Figure 11: Calculated RAP (4 hrs) for simulated ICP signal ($\sigma^2 = 0.0234$). Note: variance is occurring at a higher frequency compared to real ICP data due to 40 dB noise. Constantly low RAP values (near 0) at low ICP mean that this signal would theoretically be stable.

In comparison, real ICP values have a higher calculated variance and are mostly positive. The values observed were also expected. Since the data used were from a TBI patient, (with compromised AR) RAP should be positive and the signal more prone to fluctuations.

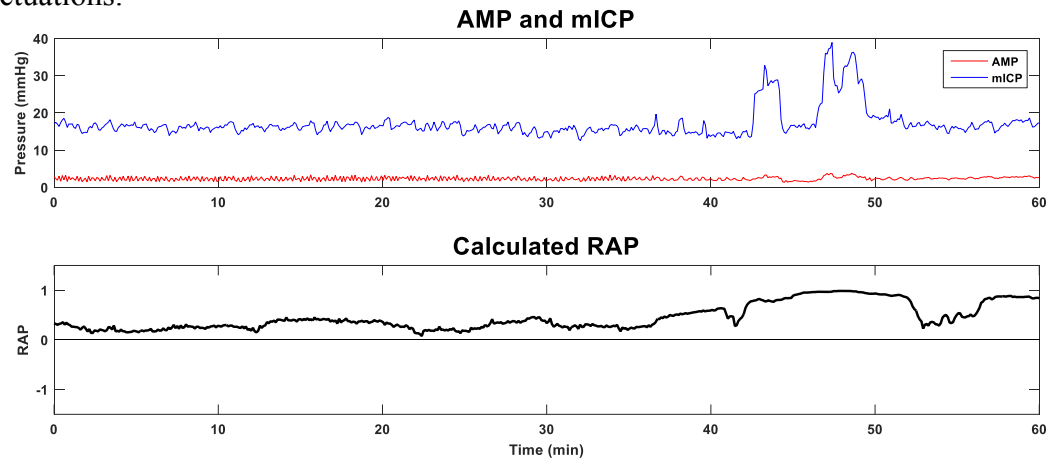

Figure 12: Calculated RAP (1 hr) for measured ICP signal from TBI patient ($\sigma^2 = 0.0675$). Higher variance observed due to unstable ICP.

II. Comparison of Stable vs. Unstable Distributions

As aforementioned, segments of data were defined as 'stable' if there were no marked events for the entire hour. Conversely, if the segment contained events, the data were defined as 'unstable'. It was observed that the probability distribution of stable vs. unstable ICP data (Fig. 13a) did not seem to differ in terms of position with values in the same region. However, stable ICP data contained a higher density of stable values (~15 mmHg) in comparison to unstable data which was expected. Based on the distribution results, it is difficult to tell whether ICP is stable or unstable by using a threshold. However, since it has been previously determined that using the clinical ICP threshold of $\geq$ 20 mmHg increases the probability of good outcome, this threshold was used instead [51]. On the other hand, though there is some overlap, there is a clear shift in RAP for stable vs. unstable values (Fig. 13). Thus, a RAP threshold (0.5) can be used to differentiate between stable vs. unstable with 83.4% reliability (Appendix D).

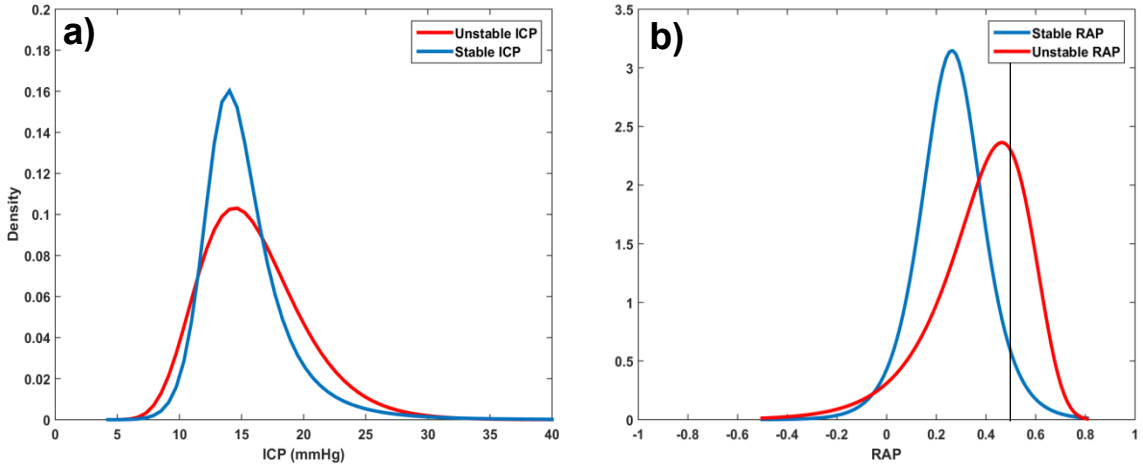

Figure 13: a) Probability distribution of unstable (red) vs. stable (blue) ICP data. b) Probability distribution of unstable (red) vs. stable (blue) RAP data. The black reference line at 0.5 marks the threshold chosen for categorizing events as unstable.

III. Latency Between RAP Increase and ICP events

For the patients investigated, the latency period between RAP and ICP events varied (≤ 5 min) but was normally 1-3 min. The start time was determined by the point at which RAP exceeded the set threshold prior to an event while the end time was set at the ICP event. The data investigated thus far indicates that RAP has potential for forecasting (Fig. 14-5). However, more patients must be observed to calculate an average latency period. It is also possible that there are different latency periods for different types of events.

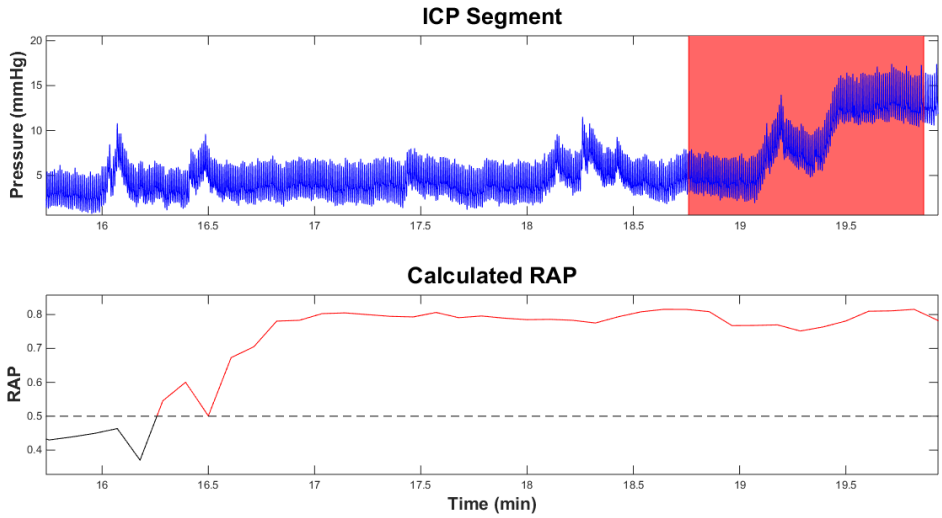

Figure 14: Patient 2, Hr 7 – RAP crosses the threshold and stays positive approx. 3 minutes before an event occurs in ICP.

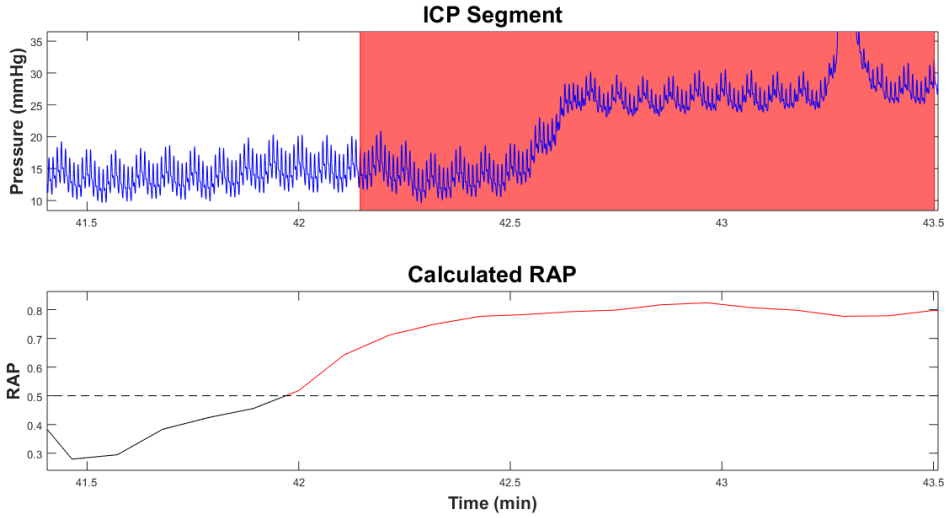

Figure 15: Patient 1, Hr 25 – RAP crosses the threshold approx. 30 seconds prior to the event

IV. ICP vs. RAP

The compensatory reserve plot (CRP) of ICP vs. RAP has been marked with the previously determined RAP threshold of 0.5 and the clinical threshold of 20 mmHg. The interpretation of the CRP is described in figure 16.

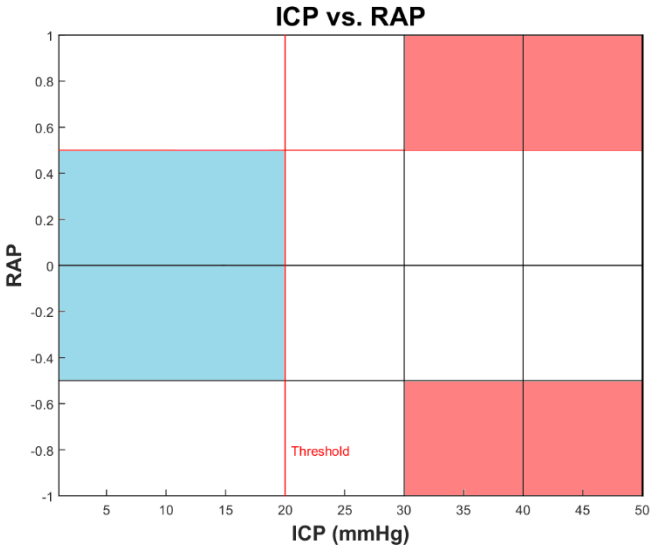

Figure 16: The CRP has been separated into regions based on thresholds demarcated by the red lines. Any values in the red regions mean that the patient is very unstable (due to high values of ICP coupled with a high RAP magnitude). Values in the blue region mean that the patient is most likely stable (due to low ICP coupled with low amplitude values) [32, 34]. Values in any other areas are indeterminate

i. Simulated ICP Data

Figure 17 shows the CRP for an hour of simulated ICP data. The CRP of simulated ICP data shows expected values. It can be seen that the ICP and RAP stay within stable regions (Fig. 17b). Note that the mean does not lie in the center of the shown ICP range (see Fig. 10a)

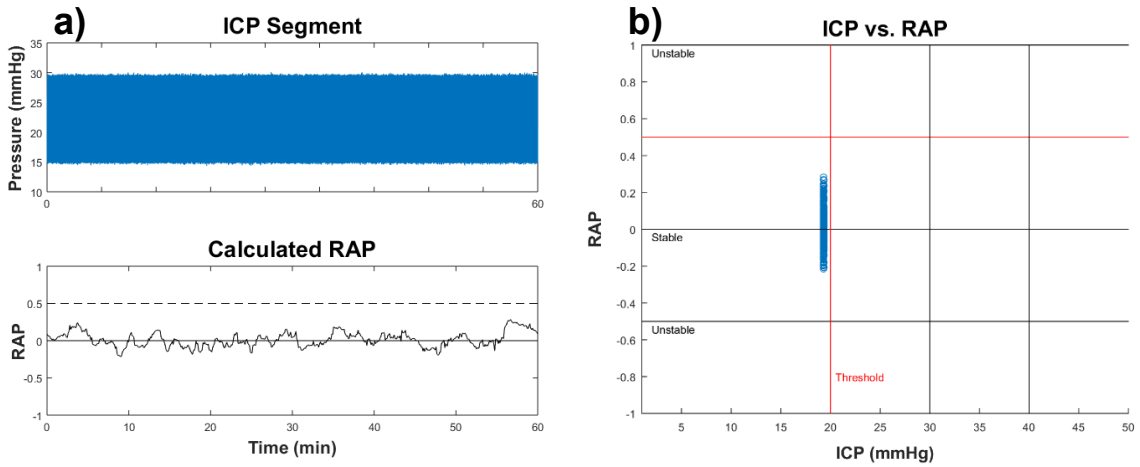

Figure 17: a) 1 hour of simulated ICP and calculated RAP values, b) CRP of ICP vs. RAP values for simulated ICP in (a)

ii. Hours 22-24 : ICP vs. RAP in TBI Patient 1

Figure 18 shows how ICP and RAP (22^{nd} -24^{th} hour) vary before, during, and after an event has occurred. In the 22^{nd} hour (Fig 18a-b), ICP and RAP are relatively constant. The CRP also shows that points stay densely packed within the stable regions. When the event occurs in the 23^{rd} hour (Fig 18c-d) data points spread out into the unstable regions with most points still in the stable region. After the event (Fig 18e-f), data is closer to the thresholds and less densely packed, but mostly within the stable region.

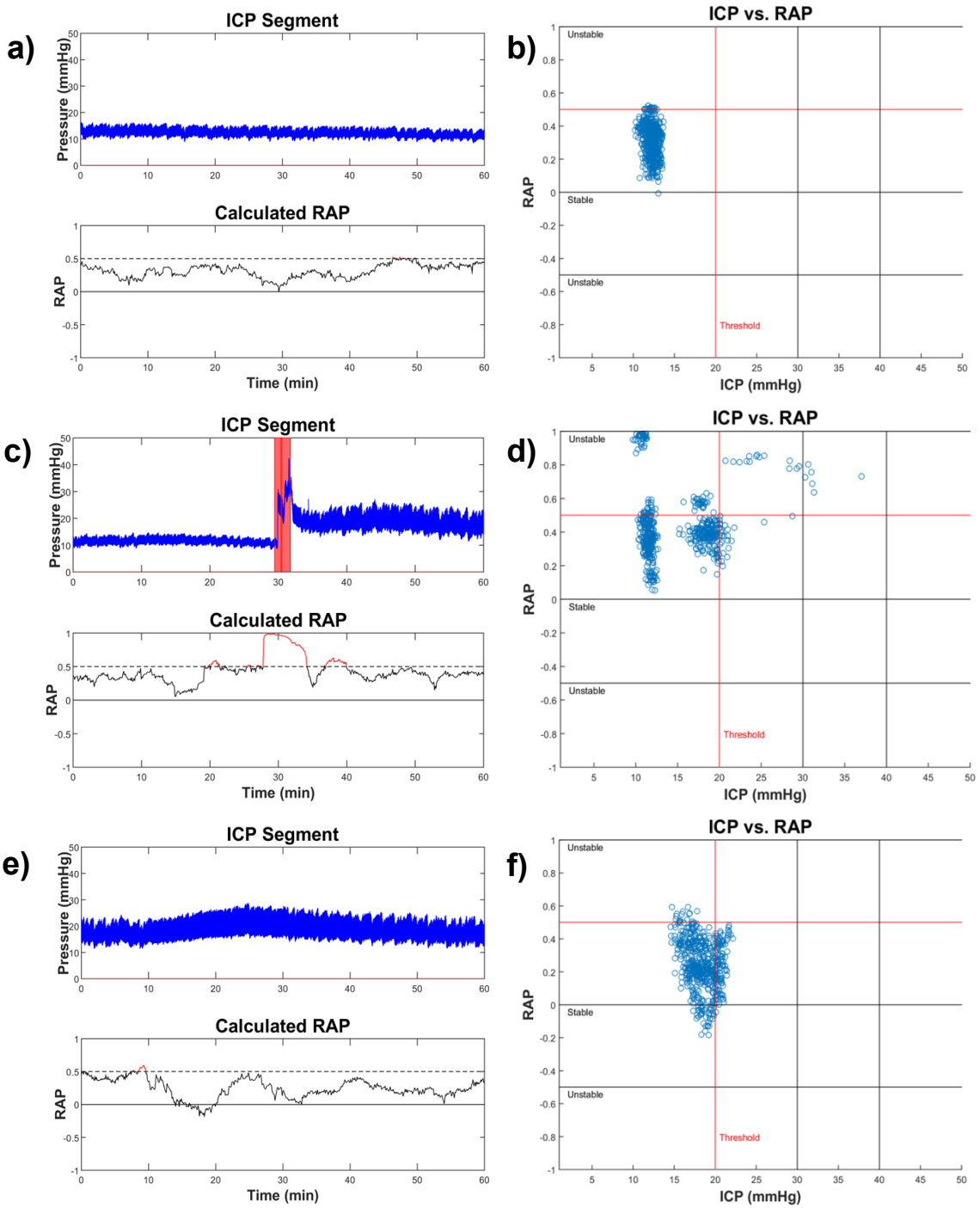

Figure 18: Patient 1;3 – 1 hour consecutive segments from 22nd -24th hours shows the distribution ICP and RAP before (a-b), during (c-d), and after (e-f) an unstable period. (a,c,e) 0.5 RAP threshold shown as dotted line with unstable RAP in red. Note: ICP data down-sampled to size of RAP for CRPs.

iii. Subsequent Hours 25-27 : ICP vs. RAP in Patient 1

Figure 19 is composed of the subsequent three hour timespan in the same patient, but here it can be observed that after the event (Fig. 19c-d), RAP remains high despite what appear to be low, stable ICP values. This could mean that although the patient's ICP appears to have stabilized, their AR is still compromised for at least an hour after the event has occurred. In contrast to figure 18, there is a larger density of high RAP values in unstable regions in figure 19a-b. This is could be a cause, but further study needs to be done before making any conclusions. When RAP values finally stabilize in the 27th hour, the points shift back to the stable region (Fig 19e-f).

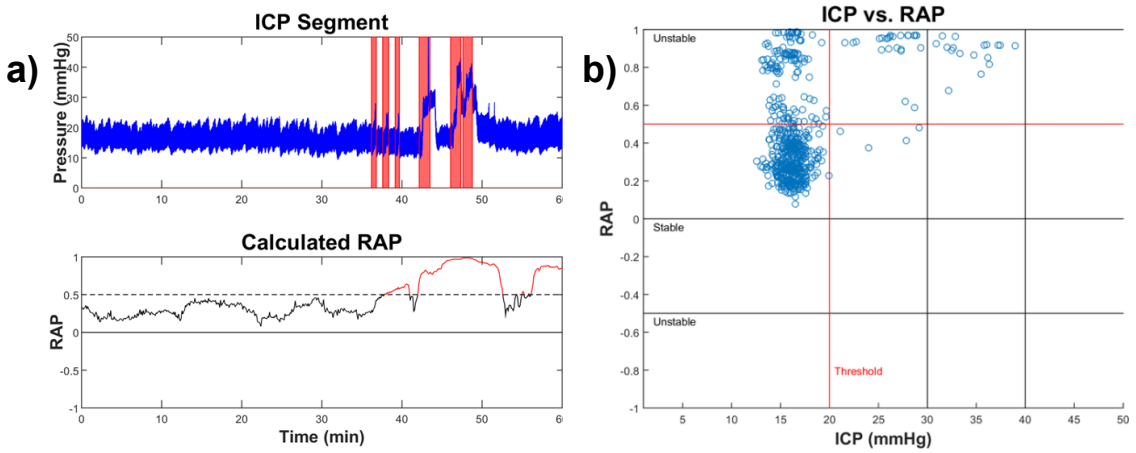

Figure 19: Patient 1;Subsequent 3 hour timespan (25th -27th) shows stabilization 2 hours after an event (a-b). (c-d) illustrate that despite the appearance of low stable ICP, RAP values may stay high for a prolonged period before stable RAP values are reached (e-f)

Figure 19 cont'd

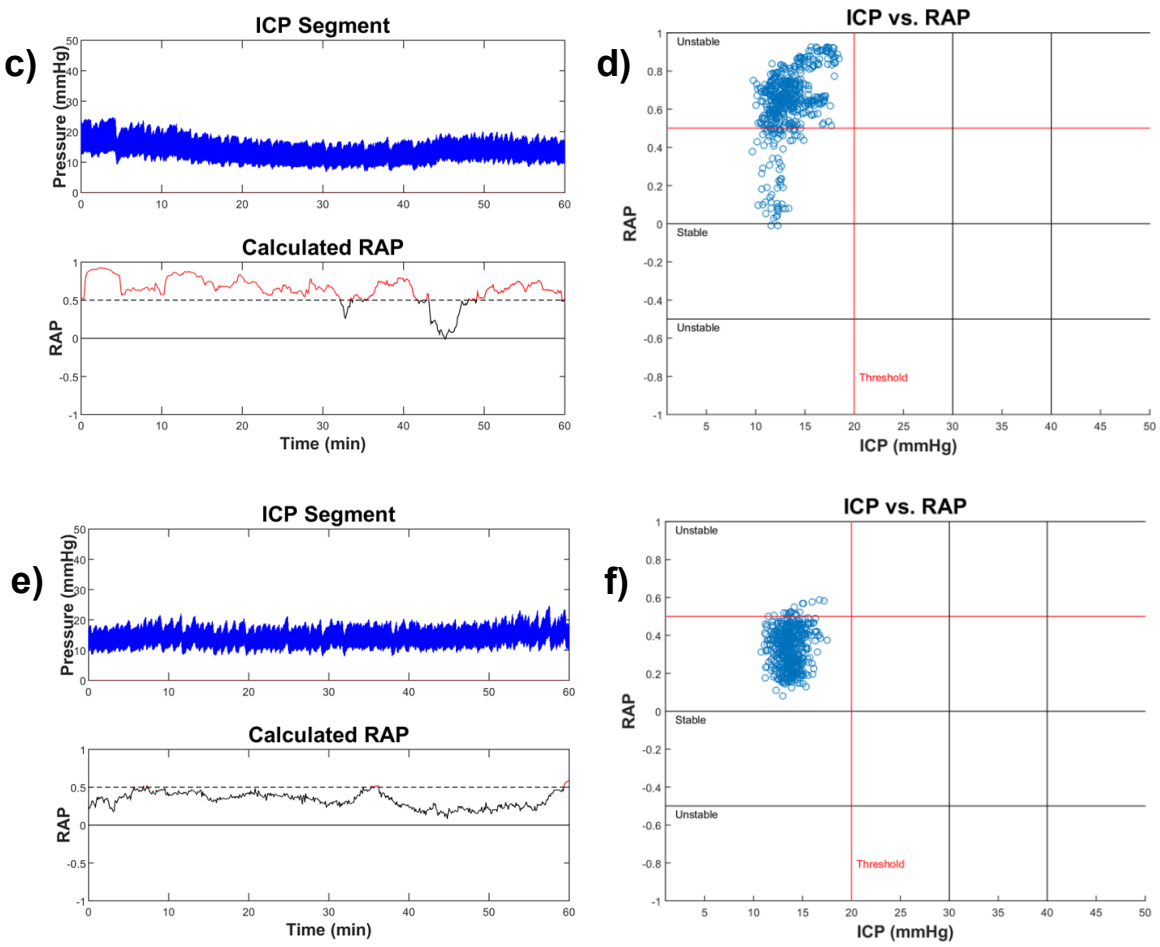

iv. Hours 62-63 : ICP vs. RAP in TBI Patient 2

Analysis of patient 2 during hours 61-63 reveals both similarities and differences with results from patient 1. During hour 61 (Fig. 20a), a sudden spike in ICP closely follows a transient rise in RAP – appearing to predict rise in ICP as a transient (3-4 min) event. RAP then declined (and reached negative values) while ICP remained elevated until hour 62 (Fig. 20c- d). This contrasts with behavior observed in patient 1 (Fig. 19) where RAP remains above the threshold despite low ICP values. Looking at RAP alone, what is observed in figure 20 could mean one of two things – either AR is about to be lost or AR remains intact despite high ICP. When ICP is taken into account, it can be

concluded that the latter applies (since ICP returns to normal levels after 30-40 min). In addition, no events occur until hour 67. In the case of both patient 1 and 2 it becomes clear that RAP does not just follow the ICP trend but is sensitive to factors other than the ICP level.

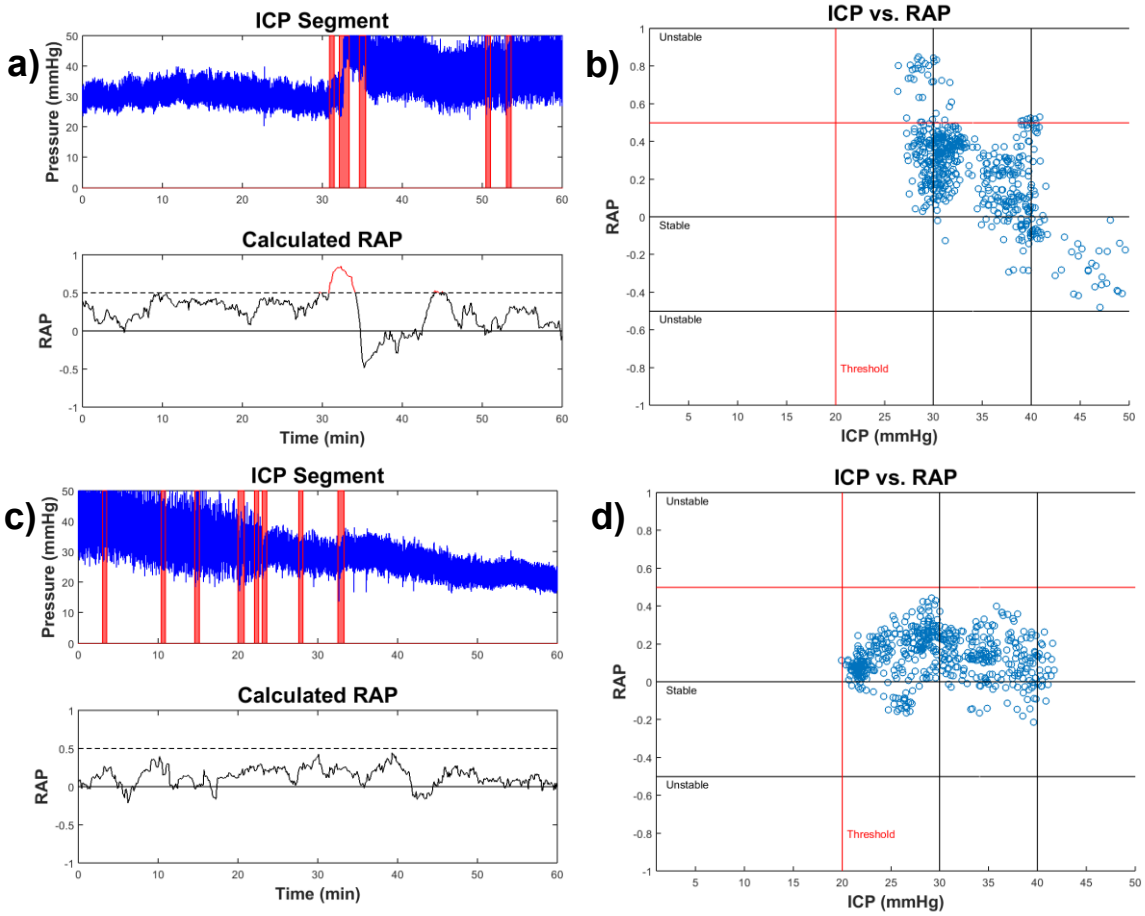

Figure 20: Patient 2; 3 hour timespan (61st -63rd) shows ICP and RAP before (a-b), during and after an event (a-b). Increased ICP is observed with low RAP, but ICP decreases after the event (c-d) and RAP maintains mostly positive values for subsequent hours with no event up to the 67th hour (c-f)

Figure 20 cont'd

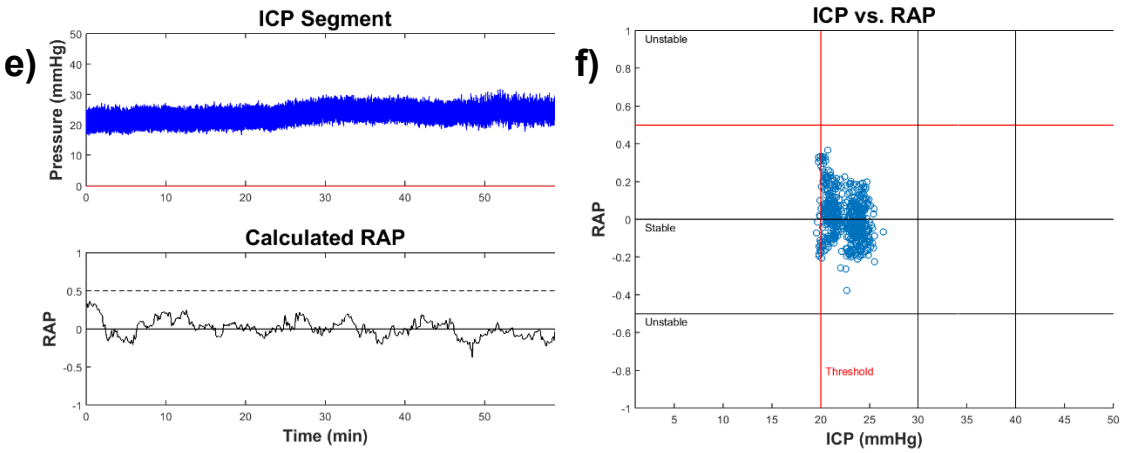

v. Hours 127-129 : ICP vs. RAP in TBI Patient 2

Figure 21 presents another scenario where high ICP accompanies high RAP. As aforementioned, this type of pairing is expected for patients with TBI and indicates compromised AR (Fig. 21c-d). It can be further observed that in the minutes prior to the event, average RAP exceeds the threshold and gradually increases despite low ICP (Fig. 21a-b). Note that the lack of continuity is because RAP was calculated separately for each hour segment instead of continuously to ease processing. Again, it can be seen that after the events in hour 128, RAP remains high, but then stabilizes along with ICP (Fig. 21e-f).

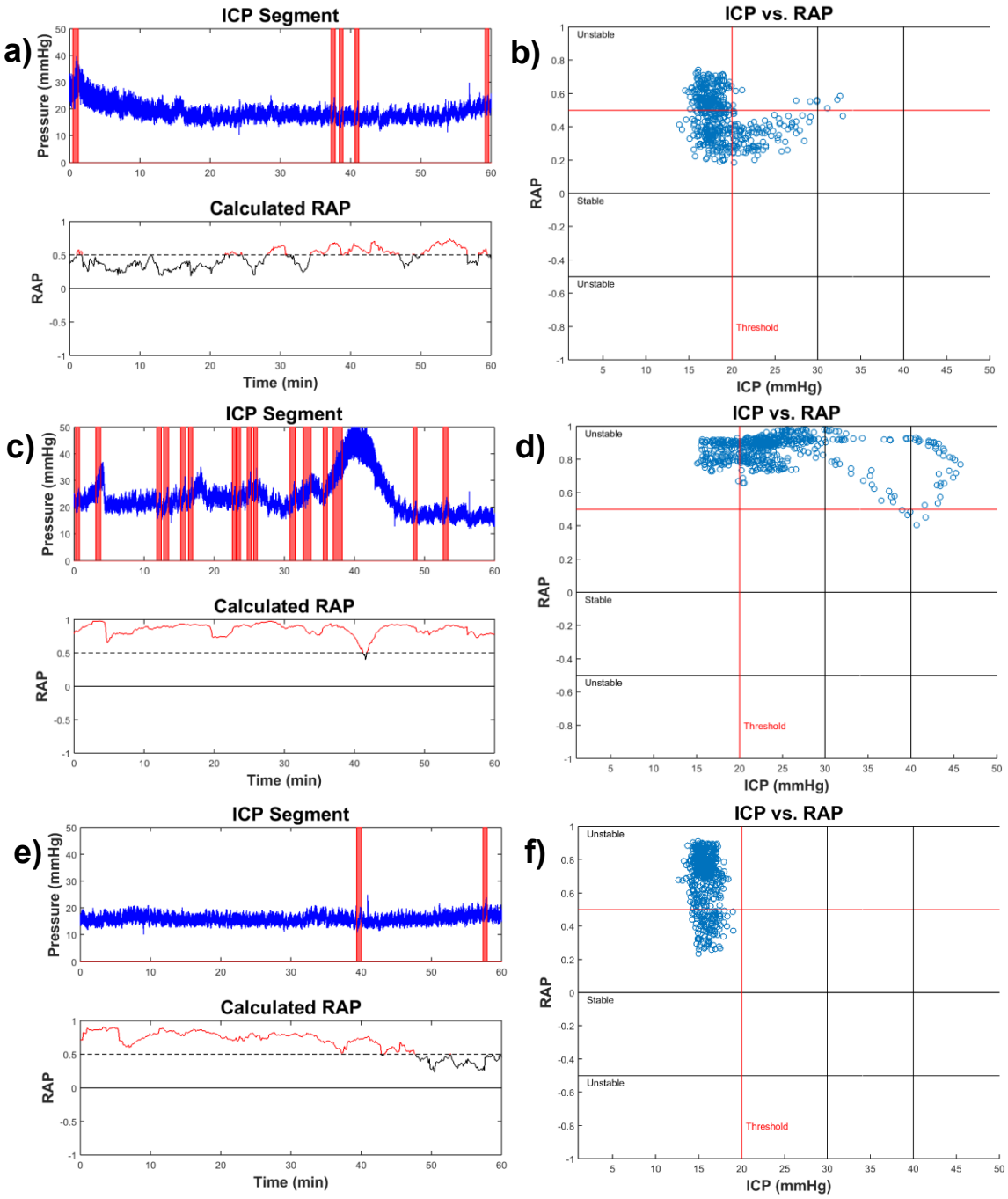

Figure 21: Patient 2; 3 hour timespan (127th -129th) shows increase in RAP despite low ICP prior to event (a-b) consistently high RAP during the event (c-d) and delayed RAP stabilization as ICP decreases below threshold after the event (e-f

V. Mean vs. Amplitude of ICP

The mean vs. amplitude (mICP vs. AMP) plots showed low correlation throughout for both patients 1 and 2 (< 0.25). Only one breakpoint (change from positive to negative) was observed in the entire length of the data for both patients 1 and 2. As mentioned, breakpoints have previously been found as indicators of patient outcome. Sometimes the presence of a breakpoint correlated with a fatal outcome [32, 34]. However, no conclusion can be made here since both patients did not have fatal outcome with only one breakpoint observed for each patient. Figures 22-3 show the observed breakpoints for each patient. The breakpoints observed also represent a small change in slope while in literature the difference was higher (0.53 to – 0.358) for a fatal outcome [32]. Regardless, further research needs to be conducted on more patients with different outcomes to find what values would be indicative of fatal vs. good outcome.

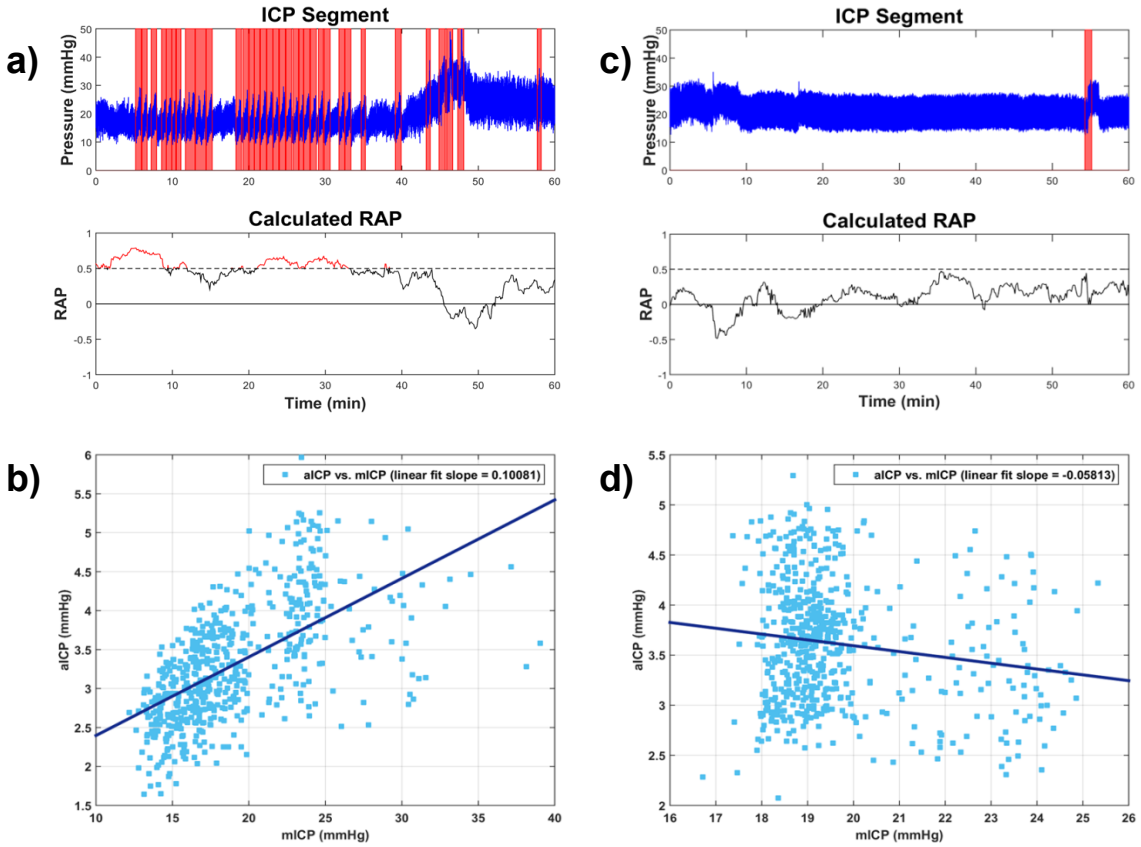

Figure 22: Patient 1; 2 consecutive hours where a breakpoint or change from positive (a-b) to negative (c-d) slope, was found in plotted amplitude vs. mean ICP data. (a) 14th hour ICP and RAP data (b) amplitude and mean ICP data from that hour plotted against each other with a linear fit; slope = 0.10081 (c) 15th hour ICP and RAP data (d) amplitude and mean ICP data from that hour plotted against each other with a linear fit; slope = -0.05813

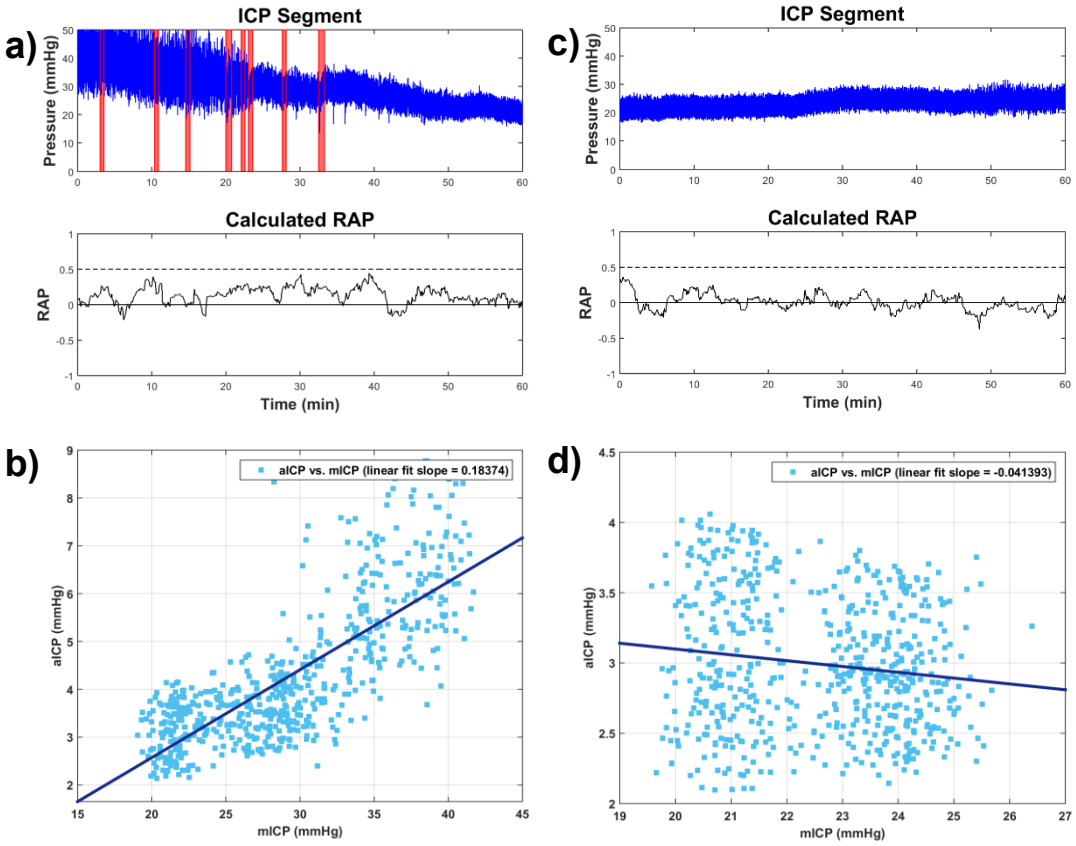

Figure 23: Patient 2; 2 consecutive hours where a breakpoint or change from positive (a-b) to negative (c-d) slope, was found in plotted amplitude vs. mean ICP data. (a) 62nd hour ICP and RAP data (b) amplitude and mean ICP data from that hour plotted against each other with a linear fit; slope = 0.18374 (c) 63rd hour ICP and RAP data (d) amplitude and mean ICP data from that hour plotted against each other with a linear fit; slope = -0.041393

Future Work

As previously discussed, further research for this project will need to include more patients for comparison. Since RAP is a normalized value, this should make it easier to compare between patients whereas mICP varies from patient to patient [32]. Data can be obtained from more SICU patients or via existing databases. The next step would be to find trends in ICP vs. RAP data. This can be done by quantifying and comparing the density/location of ICP vs. RAP points before, during, and after events. After categorizing the data, the distribution and location of points can be compared for several stacked events to see whether points tend to lie in specific regions, etc. When a sufficient number of patients/outcomes have been obtained, then RAP values (and breakpoints) can then be compared with patient outcome. In conjunction with the aforementioned, some further research should also be done to find the average latency between RAP and ICP events. This data can be used to determine how far ahead the index is capable of forecasting. Additionally, ICP and RAP events can be classified into categories to see whether there is a different latency period for each category. Finally, although data was collected from more than one patient for this project, the large amount of artifacts and noise has made it difficult to use much of the data. Moreover, nurses are also instructed to re-zero the ICP monitor every time something changes. This must be factored in to future data. Hence, developing a better noise/artifact filtering method is another important goal.

Conclusions

The novel findings in this study are: 1) the compensatory reserve plot (CRP) was introduced to quantify the relationship between RAP and ICP as shown in figures 18-21. CRPs codify the generally accepted notion of intracranial hemodynamic instability, whereby the degree of autoregulatory impairment is reflected in the relationship between RAP and ICP (as described by the pressure-volume curve), 2) positive RAP generally accompanied high ICP (Fig. 19a-b and 21) while low RAP accompanied low ICP (Fig 18a-b and 19e-f), 3) The RAP distribution in 'stable' states differs significantly ($p < 0.001$) from that in 'unstable' states (Fig. 13, Appendix E), and 4) in the cases examined, RAP spiked in the minutes prior to a rise in ICP. Therefore, RAP should be further investigated as a possible forecasting tool. If the RAP index is deemed to be a useful predictive index, the predictive efficacy of other indices will be compared against RAP. Once comparisons between different indices have been completed, a weighted combinatorial AR assessment algorithm will be installed in CHARM, and the growing database of SICU data will be tested to validate. After testing the AR algorithm, CHARM will be used for real-time TBI monitoring.

Appendix A

Distribution of the Derivative of ICP (dICP): Valid ICP Segments

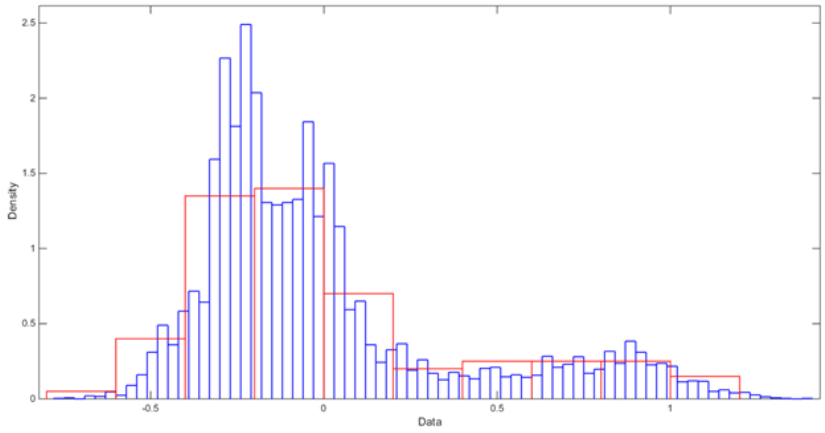

- Range of valid ICP segments: -1 to 2

Distribution of dICP: Invalid ICP Segments

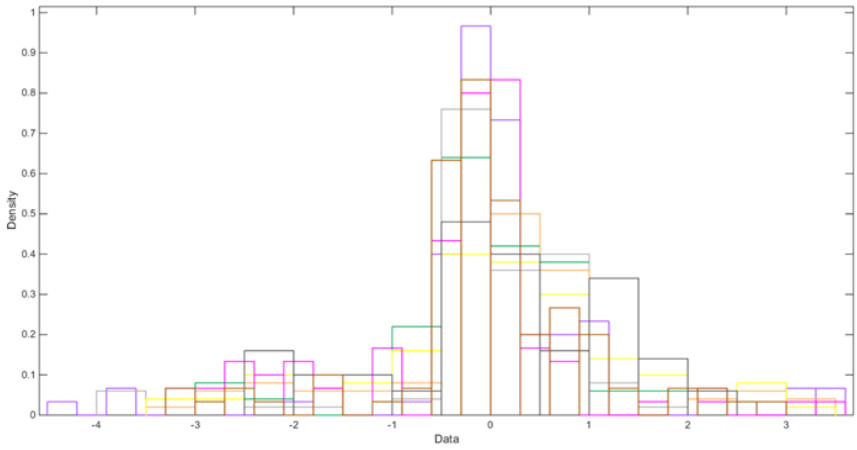

- Range of invalid ICP segments: -4.5 to 3.5

Values outside the range of valid dICP were categorized as invalid segments.

Appendix B

Method Used to Generate Simulated ICP Data

1. The following function simulating an ICP wave is repeated in Matlab:

```
ICP_Sim = 15 + 36*(A1.*exp(-k1.*(t-a1).^2) + A2.*exp(-k2.*(t-a2).^2) +
A3.*exp(-k3.*(t-a3).^2));
```

2. White Gaussian Noise was added the signal

```
t_length=linspace(0,(size(ICP_Sim_rep,2)-1)/50,size(ICP_Sim_rep,2));
ICP_Sim = awgn(ICP_Sim,40,'measured',1); %noise
ICP_Sim_rep = awgn(ICP_Sim_rep,40,'measured',1);
```

Appendix C

Matlab: Distribution Fitting Tool used to obtain fit for probability distributions of ICP and RAP data

- ICP Data: 9 hours of ICP data used for each distribution

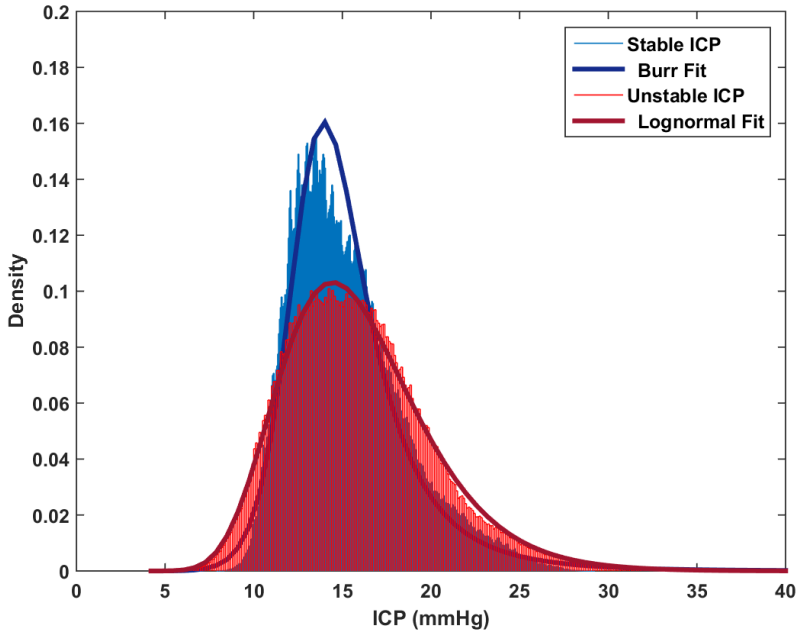

- RAP Data: 9 hours of associated RAP data used for each distribution

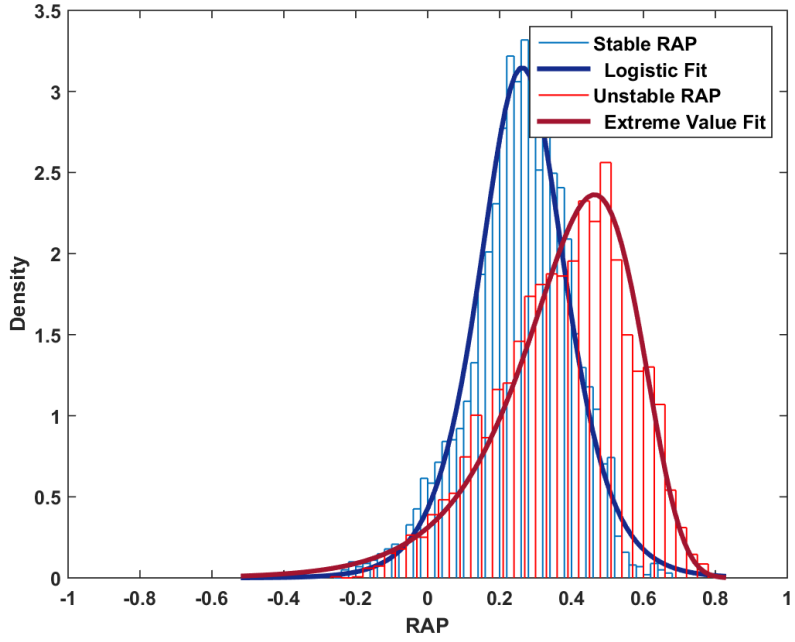

Appendix D

- Reliability Calculation
    1. Points for each of the curves were evaluated using Matlab: Distribution Fitting Tool
    2. The area underneath the unstable RAP curve from 0.5 to the end of the curve was determined
    3. Reliability = area in between the 2 curves (highlighted in yellow) / total area underneath unstable RAP curve

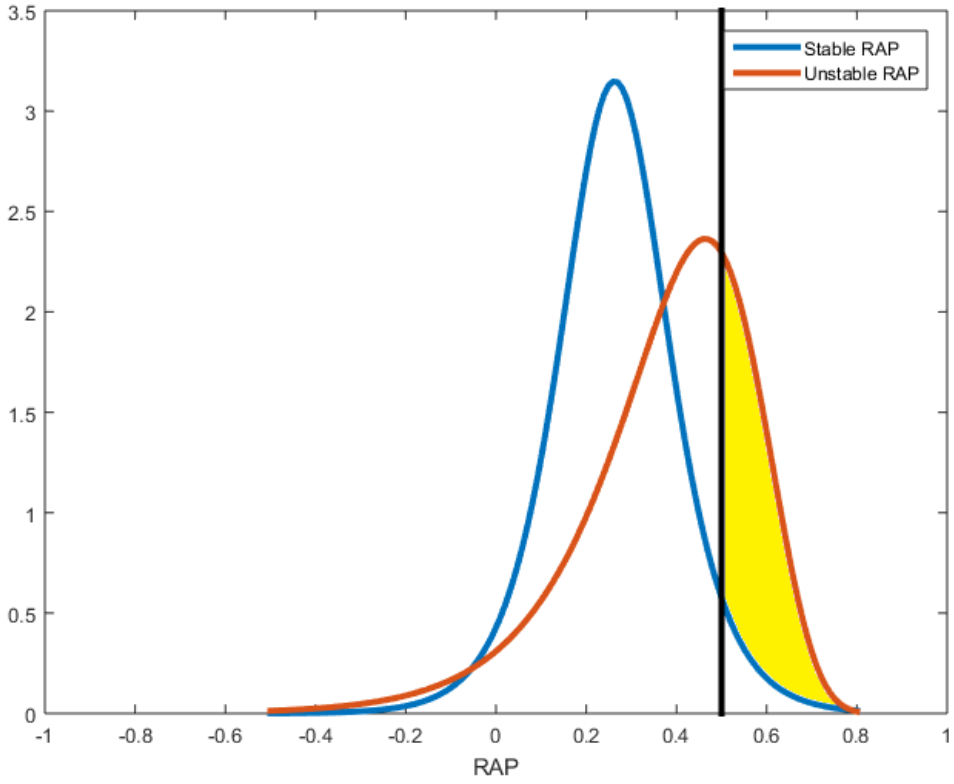

Appendix E

Statistical tests and p-values used to determine whether ‘stable’ vs. ‘unstable’ RAP values significantly differ

Test	**Null Hypothesis**	**p-value**	**Conclusion**
Mann-Whitney U test (aka Wilcoxon rank-sum test)	H_0: The 2 samples come from the same population	1.2736e-285	H_0 is rejected
2 sample Kolmogorov-Smirnov Test (KS Test)	H_0: The 2 samples come from the same distribution	4.9459e-282	H_0 is rejected
Paired t-Test	H_0: Difference between means is 0	1.7067e-231	H_0 is rejected

References

[1] Ribbers GM. 2010. Brain Injury: Long term outcome after traumatic brain injury. In: JH Stone, M Blouin, editors. International Encyclopedia of Rehabilitation. Available online: http://cirrie.buffalo.edu/encyclopedia/en/article/338/

[2] MRC CRASH Trial Collaborators. (2007). Predicting outcome after traumatic brain injury: practical prognostic models based on large cohort of international patients. *BMJ*.

[3] Tolias C and Sgouros S. 2003. "Initial Evaluation and Management of CNS Injury." Retrieved from: emedicine.medscape.com: http://emedicine.medscape.com/article/434261-overview

[4] Alzheimer's Association. (2014). *Traumatic Brain Injury*. Retrieved from alz.org : http://www.alz.org/dementia/traumatic-brain-injury-head-trauma-symptoms.asp

[5] Brain Trauma Foundation. (n.d.). *TBI Statistics: Facts About TBI in the USA*. Retrieved from braintrauma.org: http://www.braintrauma.org/tbi-faqs/tbi-statistics/

[6] Zaloshnja, E., et al., Prevalence of Long-Term Disability From Traumatic Brain Injury in the Civilian Population of the United States, 2005. Journal of Head Trauma Rehabilitation, 2008. 23(6): p. 394-400.

[7] Shahlaie, K., Zwienenberg-Lee, M., Kim, K., & Muizelaar, P. (n.d.). *Injuries to the Central Nervous System*. Retrieved from acssurgery.com: http://www.acssurgery.com/acssurgery/institutional/getChapterByIDHTML.action?bookId=ACS&chapId=part07_ch02&type=tab

[8] Kochanek PM, Carney N, Adelson PD, Ashwal S, Bell MJ, Bratton S, Carson S, Chesnut RM, Ghajar J, Goldstein B, Grant GA, Kissoon N, Peterson K, Selden NR, Tong KA, Tasker RC, Vavilala MS, Wainwright MS, Warden CR (2012) Guidelines for the Acute Medical Management of Severe Traumatic Brain Injury in Infants, Children, and Adolescents-Second Edition Introduction. Pediatric Critical Care Medicine 13 (1):S3-S6. doi:10.1097/PCC.0b013e31823f437e

[9] Gerber LM, Chiu Y-L, Carney N, Haertl R, Ghajar J (2013) Marked reduction in mortality in patients with severe traumatic brain injury Clinical article. Journal of neurosurgery 119 (6):1583-1590. doi:10.3171/2013.8.jns13276

[10] Kirkman MA, Smith M (2014) Intracranial pressure monitoring, cerebral perfusion pressure estimation, and ICP/CPP-guided therapy: a standard of care or optional extra after brain injury? British journal of anaesthesia 112 (1):35-46. doi:10.1093/bja/aet418

[11] Mokri, B. "The Monro-Kellie Hypothesis: Applications in CSF Volume Depletion." *Neurology* 56.12 (2001): 1746-748. Web.

[12] Kim, Mi Ok, Audrey Adji, Michael F. O'Rourke, Alberto P. Avolio, Peter Smielewski, John D. Pickard, and Marek Czosnyka. "Principles of Cerebral Hemodynamics When Intracranial Pressure Is Raised." *Journal of Hypertension* 33.6 (2015): 1233-241. Web.

[13] Mcilvoy, Laura, and Kimberly Meyer. "Nursing Management of Adults with Severe Traumatic Brain Injury." *AANN Clinical Practice Guideline Series* (2008): n. pag. American Association of Neuroscience Nurses / Defense and Veterans Brain Injury Center. Web. <http://www.dcoe.mil/content/navigation/documents/aann_tbi_guidelines.pdf>.

[14] Werner, C., and K. Engelhard. "Pathophysiology of Traumatic Brain Injury." *British Journal of Anaesthesia* 99.1 (2007): 4-9. Web.

[15] Sanchez-Porras, R., et al., 'Long' pressure reactivity index (L-PRx) as a measure of autoregulation correlates with outcome in traumatic brain injury patients. Acta Neurochirurgica, 2012. 154(9): p. 1575-1581.

[16] Marmarelis, V., D. Shin, and R. Zhang, Linear and nonlinear modeling of cerebral flow autoregulation using principal dynamic modes. The open biomedical engineering journal, 2012. 6: p. 42-55.

[17] Budohoski, K.P., et al., Monitoring cerebral autoregulation after head injury. Which component of transcranial Doppler flow velocity is optimal? Neurocritical Care, 2012. 17(2): p. 211-8.

[18] Johnson, U., et al., Favorable Outcome in Traumatic Brain Injury Patients With Impaired Cerebral Pressure Autoregulation When Treated at Low Cerebral Perfusion Pressure Levels. Neurosurgery, 2011. 68(3): p. 714-721.

[19] Zweifel, C., et al., Continuous Assessment of Cerebral Autoregulation With Near-Infrared Spectroscopy in Adults After Subarachnoid Hemorrhage. Stroke, 2010. 41(9): p. 1963-1968.

[20] Liu, J., et al., Tracking time-varying cerebral autoregulation in response to changes in respiratory PaCO2. Physiological Measurement, 2010. 31(10): p. 1291-1307

[21] Lee, J.K., et al., Cerebrovascular Reactivity Measured by Near-Infrared Spectroscopy. Stroke, 2009. 40(5): p. 1820-1826.

[22] Czosnyka, M., et al., Monitoring of Cerebrovascular Autoregulation: Facts, Myths, and Missing Links. Neurocritical Care, 2009. 10(3): p. 373-386

[23] Hu, X., et al., Nonlinear analysis of cerebral hemodynamic and intracranial pressure signals for characterization of autoregulation. IEEE Transactions on Biomedical Engineering, 2006. 53(2): p. 195-209.

[24] Vespa, P. (2003). *What is the Optimal Threshold for Cerebral Perfusion Pressure Following Traumatic Brain Injury?* Retrieved from Medscape: http://www.medscape.com/viewarticle/466997_

[25] Sviri, G. and D.W. Newell, Cerebral Autoregulation Following Traumatic Brain Injury. The Open Neurosurgery Journal, 2010. 3: p. 6-9.

[26] Wakeland, W., et al., Assessing the prediction potential of an in silico computer model of intracranial pressure dynamics. Critical Care Medicine, 2009. 37(3): p. 1079-1089.

[27] Lu, C.-W., et al., Complexity of intracranial pressure correlates with outcome after traumatic brain injury. Brain, 2012. 135: p. 2399-2408.

[28] Hornero, R., et al., Complex analysis of intracranial hypertension using approximate entropy. Crit Care Med, 2006. 34(1): p. 87-95.

[29] Hu, X., et al., Forecasting ICP Elevation Based on Prescient Changes of Intracranial Pressure Waveform Morphology. IEEE Transactions on Biomedical Engineering, 2010. 57(5): p. 1070-1078.
[30] Scalzo, F., et al., Bayesian tracking of intracranial pressure signal morphology. Artificial Intelligence in Medicine, 2012. 54(2): p. 115-123.
[31] Popovic, Djordje, Michael Khoo, and Stefan Lee. "Noninvasive Monitoring of Intracranial Pressure." *Noninvasive ICP*. N.p., n.d. Web. <http://www.noninvasiveicp.com/node/13>.
[32] Czosnyka, M., Guazzo, E., Whitehouse, P., Smielewski, Z., Czosnyka, P., Kirkpatrick, P., et al. (1996). Significance of Intracranial Waveform Analysis After Head Injury. Acta Nerochir (Wien).
[33] Kim, D.-J., Czosnyka, Z., Keong, N., Radolovich, D. K., Smielewski, P., Sutcliffe, M. P., et al. (2009). Index of Cerebrospinal Compensatory Reserve in Hydrocephalus. Neurosurgery-Online.
[34] Balestreri, M., M. Czosnyka, L. A. Steiner, E. Schmidt, P. Smielewski, B. Matta, and J. D. Pickard. "Intracranial Hypertension: What Additional Information Can Be Derived from ICP Waveform after Head Injury?"*Acta Neurochirurgica* 146.2 (2004): 131-41. Web.
[35] Budohoski, Karol P., Bernhard Schmidt, Peter Smielewski, Magdalena Kasprowicz, Ronny Plontke, John D. Pickard, Jurgen Klingelhöfer, and Marek Czosnyka. "Non-Invasively Estimated ICP Pulse Amplitude Strongly Correlates with Outcome After TBI." *Acta Neurochirurgica Supplementum Intracranial Pressure and Brain Monitoring XIV* (2012): 121-25. Web.
[36] Timofeev, Ivan, Marek Czosnyka, Jurgens Nortje, Peter Smielewski, Peter Kirkpatrick, Arun Gupta, and Peter Hutchinson. "Effect of Decompressive Craniectomy on Intracranial Pressure and Cerebrospinal Compensation following Traumatic Brain Injury." *Journal of Neurosurgery* 108.1 (2008): 66-73. Web.
[37] Steiner, L. A., M. Balestreri, A. J. Johnston, J. P. Coles, P. Smielewski, J. D. Pickard, D. K. Menon, and M. Czosnyka. "Predicting the Response of Intracranial Pressure to Moderate Hyperventilation." *Acta Neurochir (Wien) Acta Neurochirurgica* 147.5 (2005): 477-83. Web.
[38] Kim, N. (2014). Progress Report: Data Acquisition. Piscataway, NJ: Rutgers University.
[39] Czosnyka, M., and J. D. Pickard. "Monitoring and Interpretation of Intracranial Pressure." *Neuroscience for Neurologists* (2006): 285-313. Web
[40] Eide, Per Kristian, and Wilhelm Sorteberg. "An Intracranial Pressure-derived Index Monitored Simultaneously from Two Separate Sensors in Patients with Cerebral Bleeds: Comparison of Findings." *BioMedical Engineering OnLine BioMed Eng OnLine* 12.1 (2013): 14. Web.
[41] Carrera, Emmanuel, Dong-Joo Kim, Gianluca Castellani, Christian Zweifel, Zofia Czosnyka, Magdalena Kasprowicz, Peter Smielewski, John D. Pickard, and Marek Czosnyka. "What Shapes Pulse Amplitude of Intracranial Pressure?" *Journal of Neurotrauma* 27.2 (2010): 317-24. Web.

[42] Schuhmann, Martin U., Sandeep Sood, James P. Mcallister, Matthias Jaeger, Steven D. Ham, Zofia Czosnyka, and Marek Czosnyka. "Value of Overnight Monitoring of Intracranial Pressure in Hydrocephalic Children." *Pediatric Neurosurgery* 44.4 (2008): 269-79. Web.

[43] Weerakkody, R. A., M. Czosnyka, M. U. Schuhmann, E. Schmidt, N. Keong, T. Santarius, J. D. Pickard, and Z. Czosnyka. "Clinical Assessment of Cerebrospinal Fluid Dynamics in Hydrocephalus. Guide to Interpretation Based on Observational Study." *Acta Neurologica Scandinavica* 124.2 (2011): 85-98. Web.

[44] Czosnyka, M., D. J. Price, and M. Williamson. "Monitoring of Cerebrospinal Dynamics Using Continuous Analysis of Intracranial Pressure and Cerebral Perfusion Pressure in Head Injury." *Acta Neurochir Acta Neurochirurgica* 126.2-4 (1994): 113-19. Web.

[45] Howells, Tim, Anders Lewén, Mattias K. Sköld, Elisabeth Ronne-Engström, and Per Enblad. "An Evaluation of Three Measures of Intracranial Compliance in Traumatic Brain Injury Patients." *Intensive Care Med Intensive Care Medicine* 38.6 (2012): 1061-068. Web.

[46] Shahsavari, Sima, Tomas Mckelvey, Thomas Skoglund, and Catherine Eriksson Ritzèn. "A Comparison between the Transfer Function of ABP to ICP and Compensatory Reserve Index in TBI." *Acta Neurochirurgica Supplements Acta Neurochirurgica Supplementum* (2008): 9-13. Web.

[47] Czosnyka, Marek, Peter Smielewski, Ivan Timofeev, Andrea Lavinio, Eric Guazzo, Peter Hutchinson, and John D. Pickard. "Intracranial Pressure: More Than a Number." *Neurosurgical FOCUS* 22.5 (2007): 1-7. Web.

[48] Czosnyka, M., L. Steiner, M. Balestreri, E. Schmidt, P. Smielewski, P. J. Hutchinson, and J. D. Pickard. "Concept of "true ICP" in Monitoring and Prognostication in Head Trauma." *Intracranial Pressure and Brain Monitoring XII Acta Neurochirurgica Supplementum* (2005): 341-44. Web.

[49] Eide, Per, Angelika Sorteberg, Torstein R. Meling, and Wilhelm Sorteberg. "The Effect of Baseline Pressure Errors on an Intracranial Pressure-derived Index: Results of a Prospective Observational Study." *BioMedical Engineering OnLine BioMed Eng OnLine* 13.1 (2014): 99. Web.

[50] Steiner, L. A. "Monitoring the Injured Brain: ICP and CBF." *British Journal of Anaesthesia* 97.1 (2006): 26-38. Web.

[51] Ratanalert, Sanguansin, Nakornchai Phuenpathom, Sakchai Saeheng, Thakul Oearsakul, Boonlert Sripairojkul, and Siriporn Hirunpat. "ICP Threshold in CPP Management of Severe Head Injury Patients." *Surgical Neurology* 61.5 (2004): 429-34. Web.

[52] Smith, Martin. "Monitoring Intracranial Pressure in Traumatic Brain Injury." *Anesthesia & Analgesia* 106.1 (2008): 240-48. Web.

Acknowledgement of Previous Publications

In preparation for paper:

"RAP Index Predicts IH in TBI patients with _% Reliability"

Work previously published by author of this paper:

Pineda, B. A., M. J. Qadri, C. Kosinski, N. H. Kim, S. Danish, and W. Craelius. "Developing a Continuous Hemodynamic Autoregulation Monitor." *IEEE Xplore Digital Library*. IEEE, Apr. 2015. Web. <http://ieeexplore.ieee.org/xpl/articleDetails.jsp?arnumber=7117187&refinements%3D4226695528%26filter%3DAND%28p_IS_Number%3A7117035%29>.

Pending publication in Journal of Clinical Monitoring and Computing:

"Trending Autoregulatory Indices During Treatment for Traumatic Brain Injury"